# Supporting Information

## Polypyridyl-functionalizated alkynyl gold(I) metallaligands supported by tri- and tetradentate phosphanes

Montserrat Ferrer,[a,*] Leticia Giménez,[a] Albert Gutiérrez,[a] Joao Carlos Lima,[b] Laura Rodríguez,[a,c] Manuel Martínez,[a] Avelino Martín,[d] Rakesh Puttreddy [e] and Kari Rissanen[e]

[a] *Departament de Química Inorgànica i Orgànica, Secció de Química Inorgànica. Universitat de Barcelona, c/ Martí i Franquès 1-11 08028 Barcelona, Spain.*

[b] *LAQV-REQUIMTE, Departamento de Química, Universidade Nova de Lisboa, Monte de Caparica, Portugal.*

[c] *Institut de Nanociència i Nanotecnologia (IN$^2$UB). Universitat de Barcelona, 08028 Barcelona, Spain*

[d] *Departamento de Química Inorgánica, Campus Universitario-Edificio de Farmacia, Universidad de Alcalá, 28871 Alcalá de Henares, Spain*

[e] *Department of Chemistry, University of Jyväskylä, POB 35, 40014 Jyväskylä, Finland*

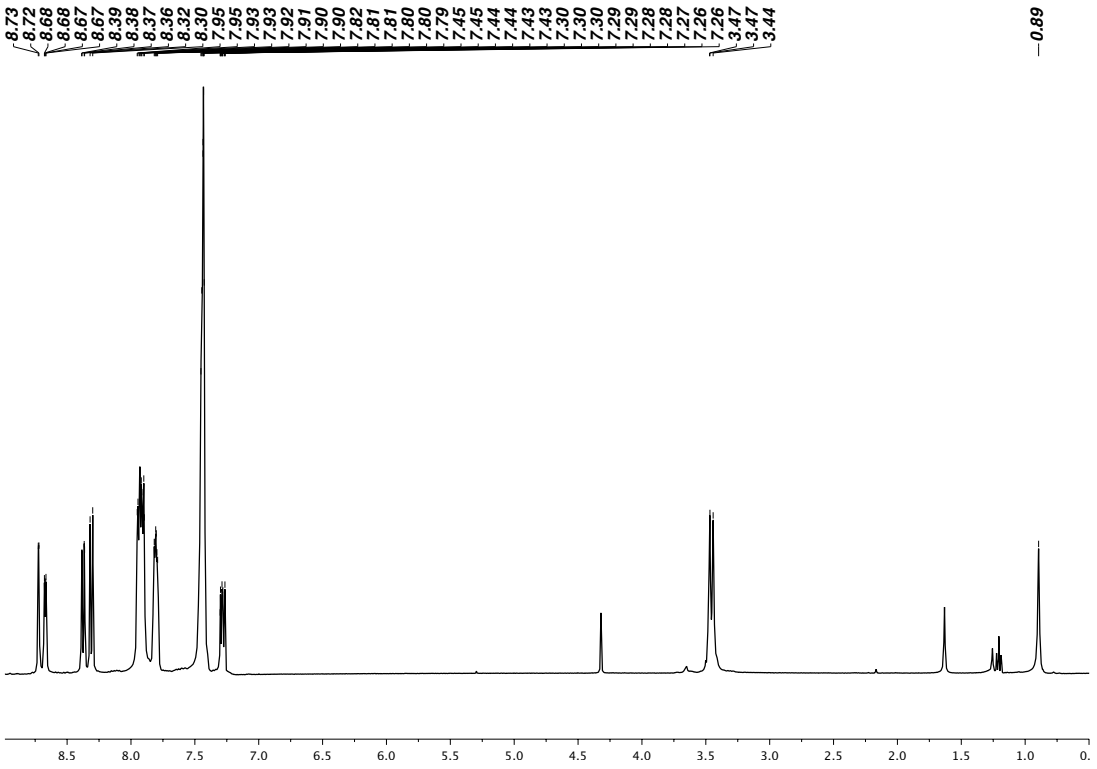


**Figure S1**. $^{1}H$ NMR of $[Au_3(C{\equiv}CC_{10}H_7N_2)_3(\mu_3\text{-triphos})]$ **(4)** in $CDCl_3$ at 298 K.

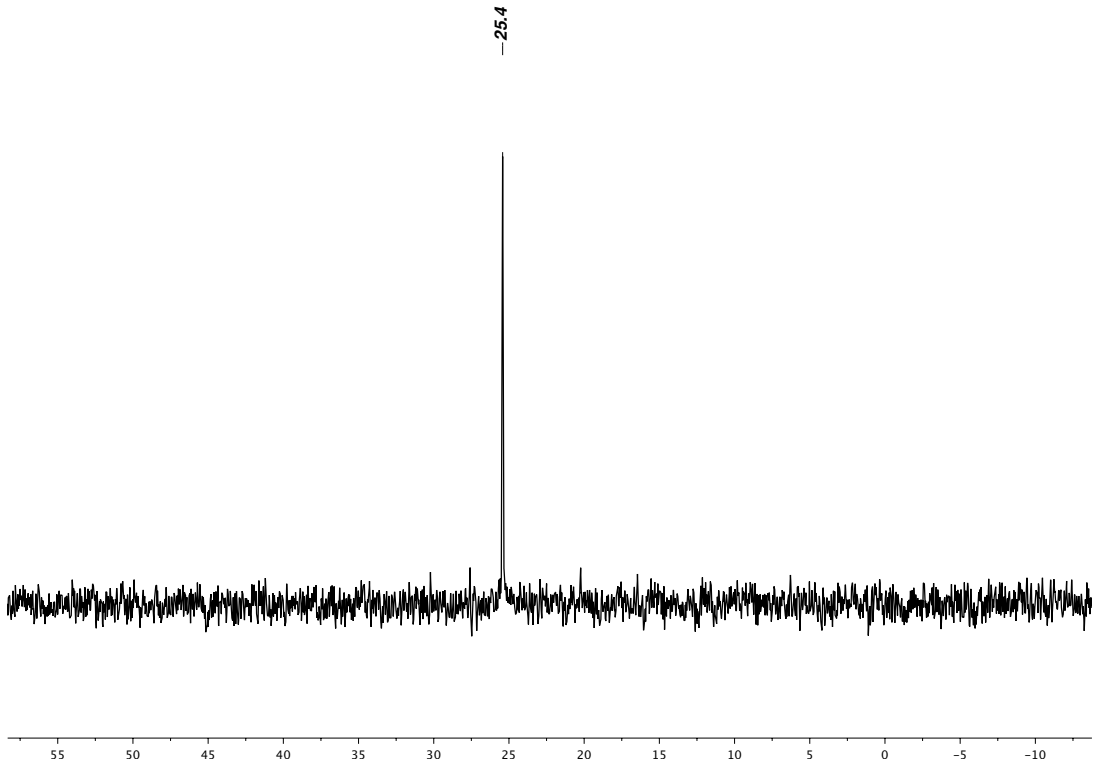


**Figure S2**. $^{31}P\{^{1}H\}$ NMR of $[Au_3(C{\equiv}CC_{10}H_7N_2)_3(\mu_3\text{-triphos})]$ **(4)** in $CDCl_3$ at 298 K.

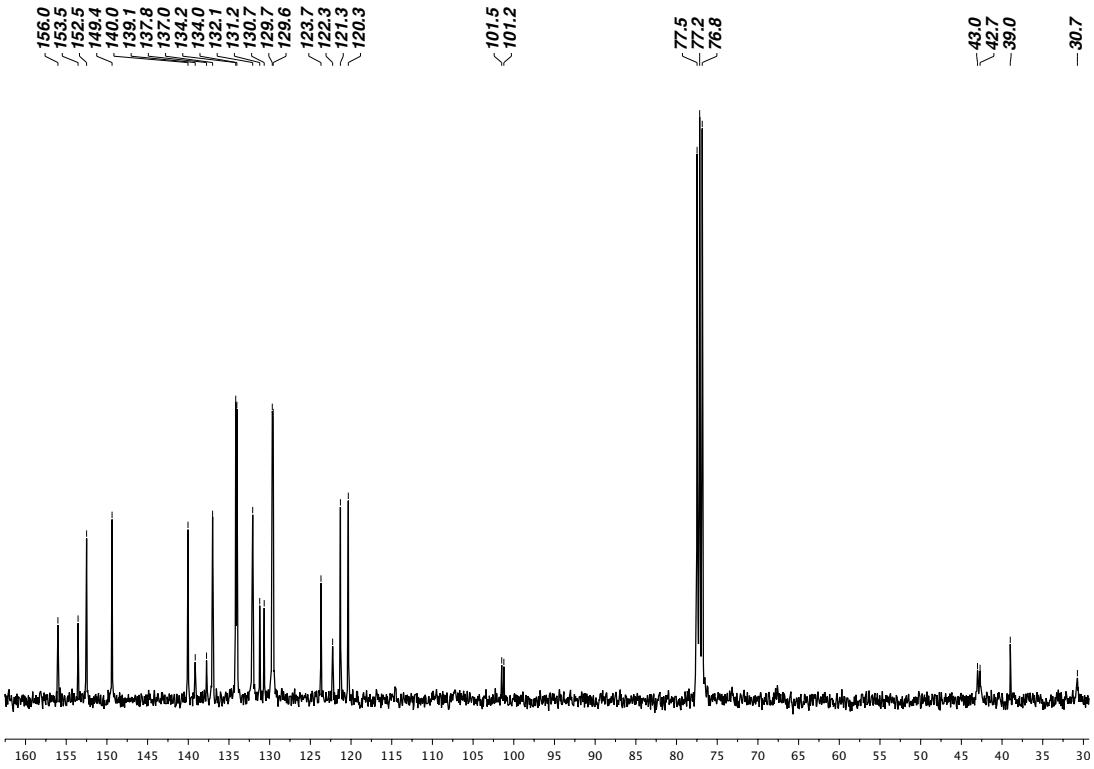


**Figure S3**. $^{13}C\{^{1}H\}$ NMR of $[Au_3(C{\equiv}CC_{10}H_7N_2)_3(\mu_3\text{-triphos})]$ **(4)** in $CDCl_3$ at 298 K.

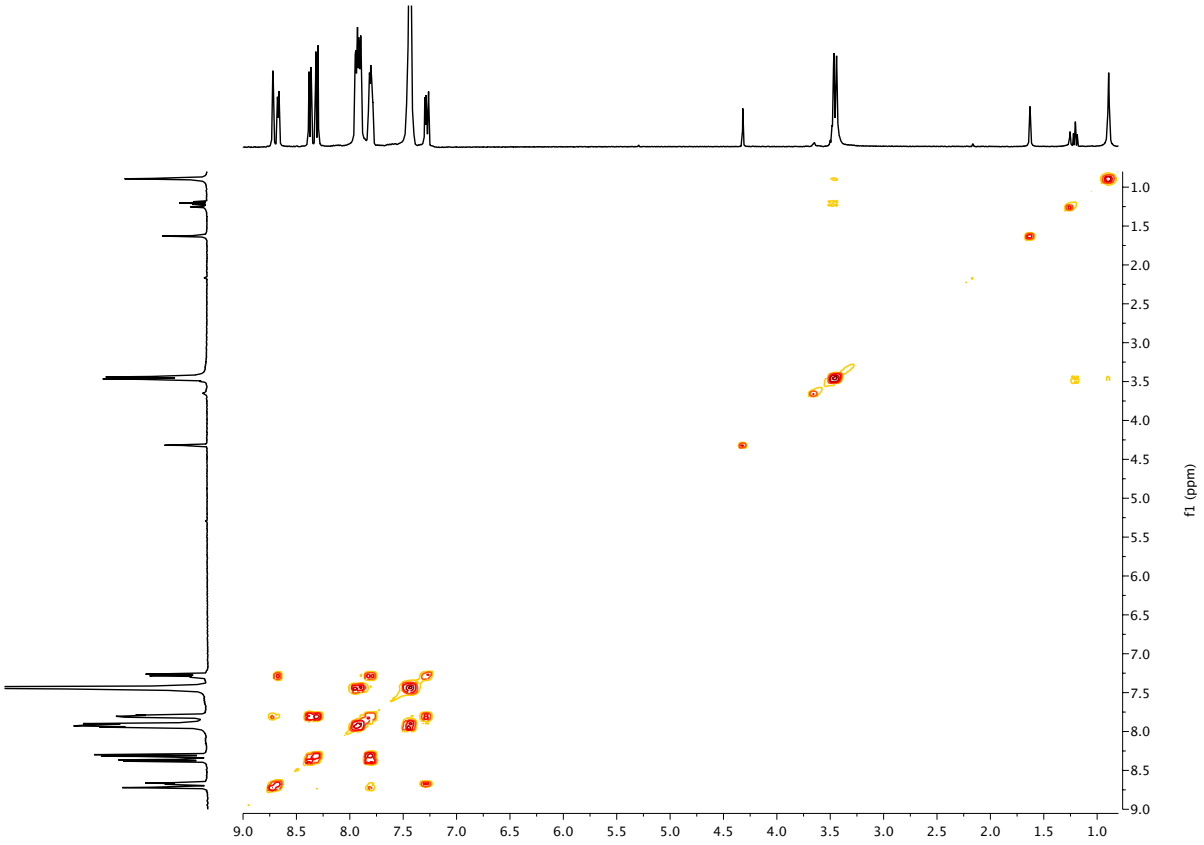


**Figure S4**. $^{1}H\text{-}^{1}H$ COSY NMR of $[Au_3(C{\equiv}CC_{10}H_7N_2)_3(\mu_3\text{-triphos})]$ **(4)** in $CDCl_3$ at 298 K.

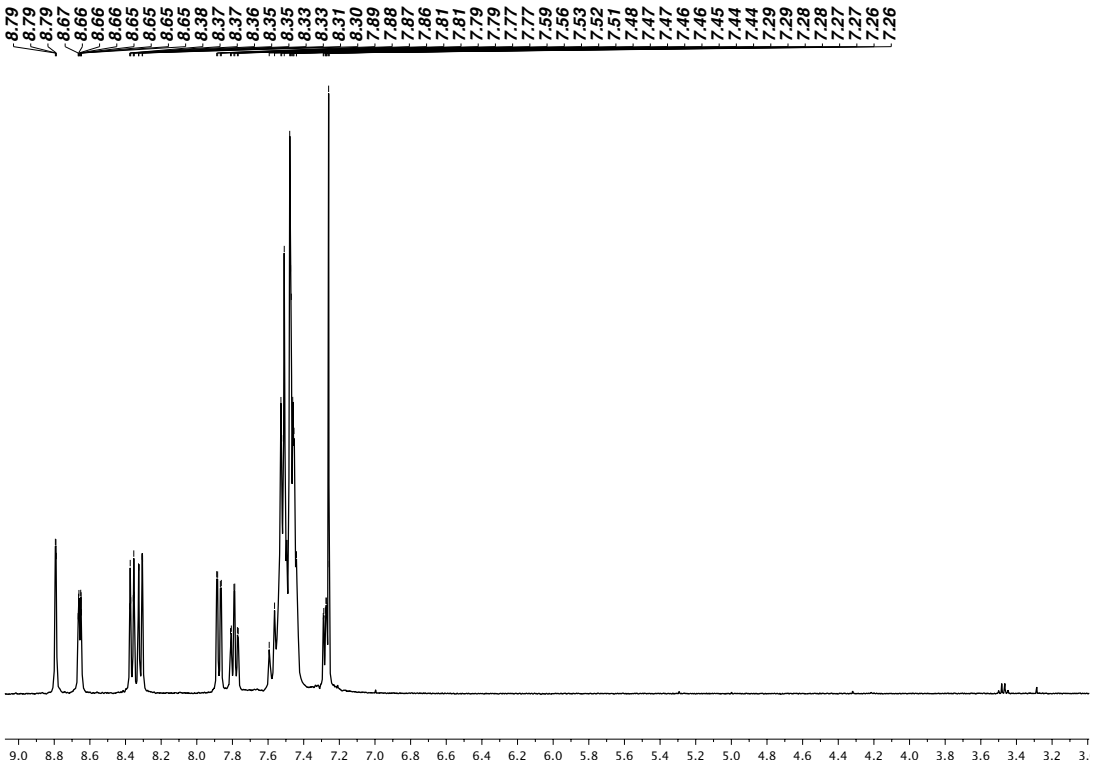


**Figure S5**. $^{1}H$ NMR of $[Au_3(C{\equiv}CC_{10}H_7N_2)_3(\mu_3\text{-triphosph})]$ **(5)** in $CDCl_3$ at 298 K.

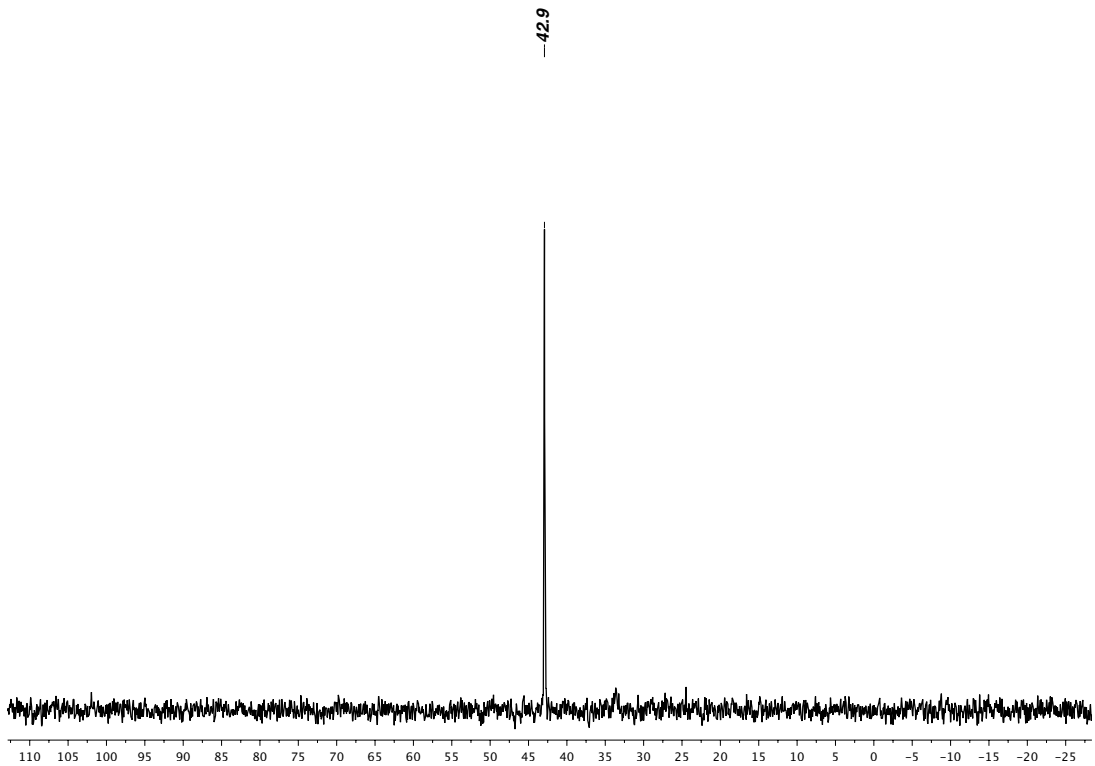


**Figure S6**. $^{31}P\{^{1}H\}$ NMR of $[Au_3(C{\equiv}CC_{10}H_7N_2)_3(\mu_3\text{-triphosph})]$ **(5)** in $CDCl_3$ at 298 K.

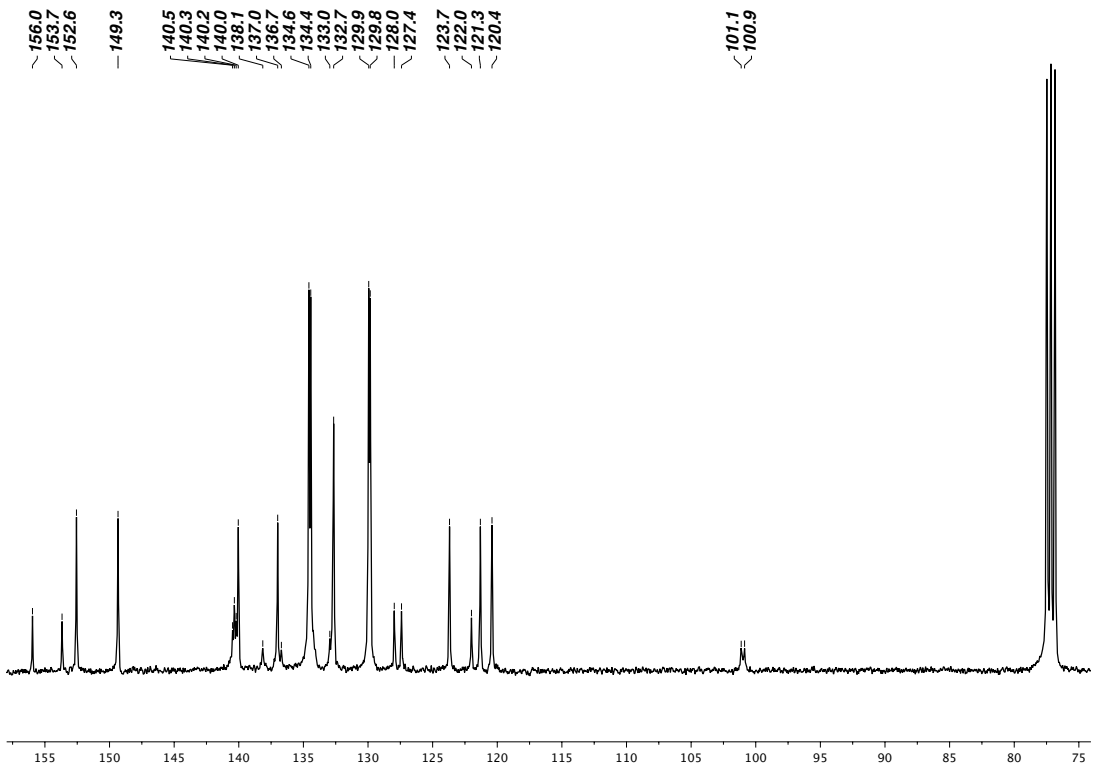


**Figure S7**. $^{13}C\{^{1}H\}$ NMR of $[Au_3(C{\equiv}CC_{10}H_7N_2)_3(\mu_3\text{-triphosph})]$ **(5)** in $CDCl_3$ at 298 K.

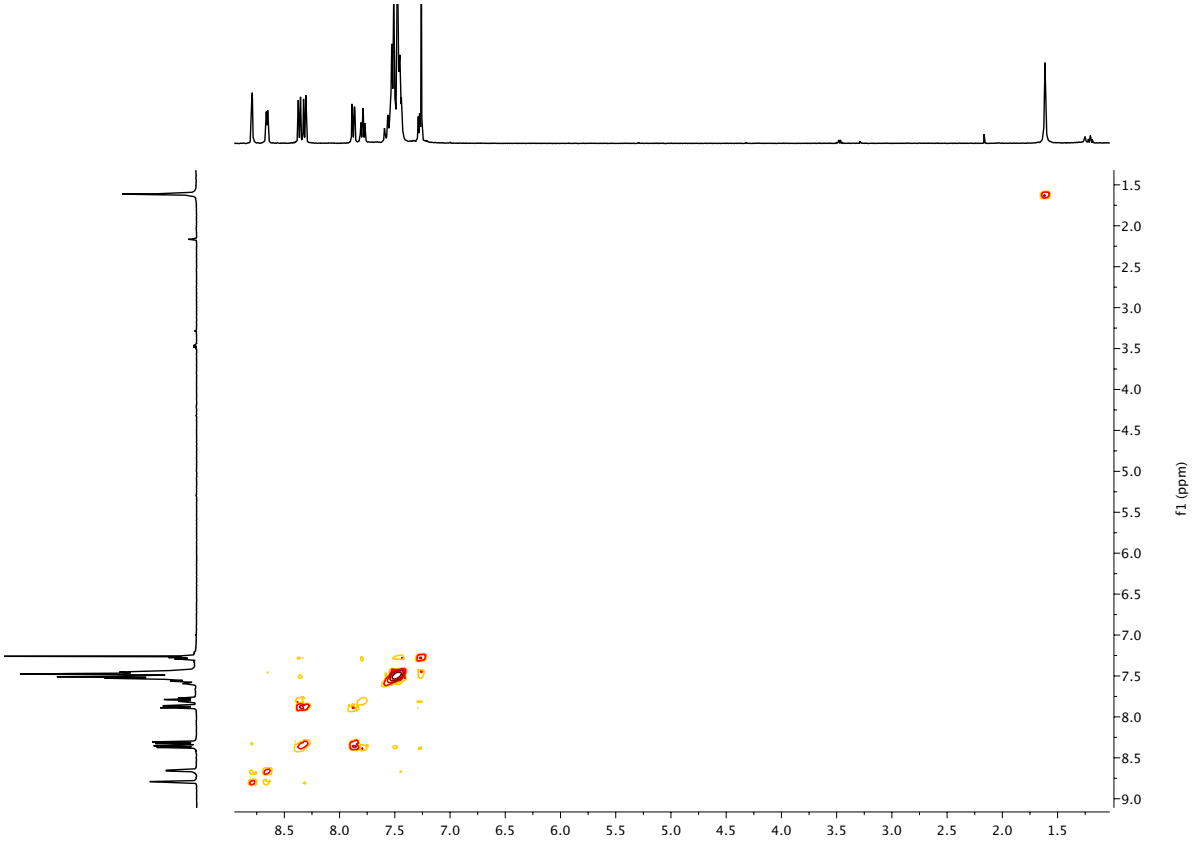


**Figure S8**. $^{1}H$-$^{1}H$ COSY NMR of $[Au_3(C{\equiv}CC_{10}H_7N_2)_3(\mu_3\text{-triphosph})]$ **(5)** in $CDCl_3$ at 298 K.

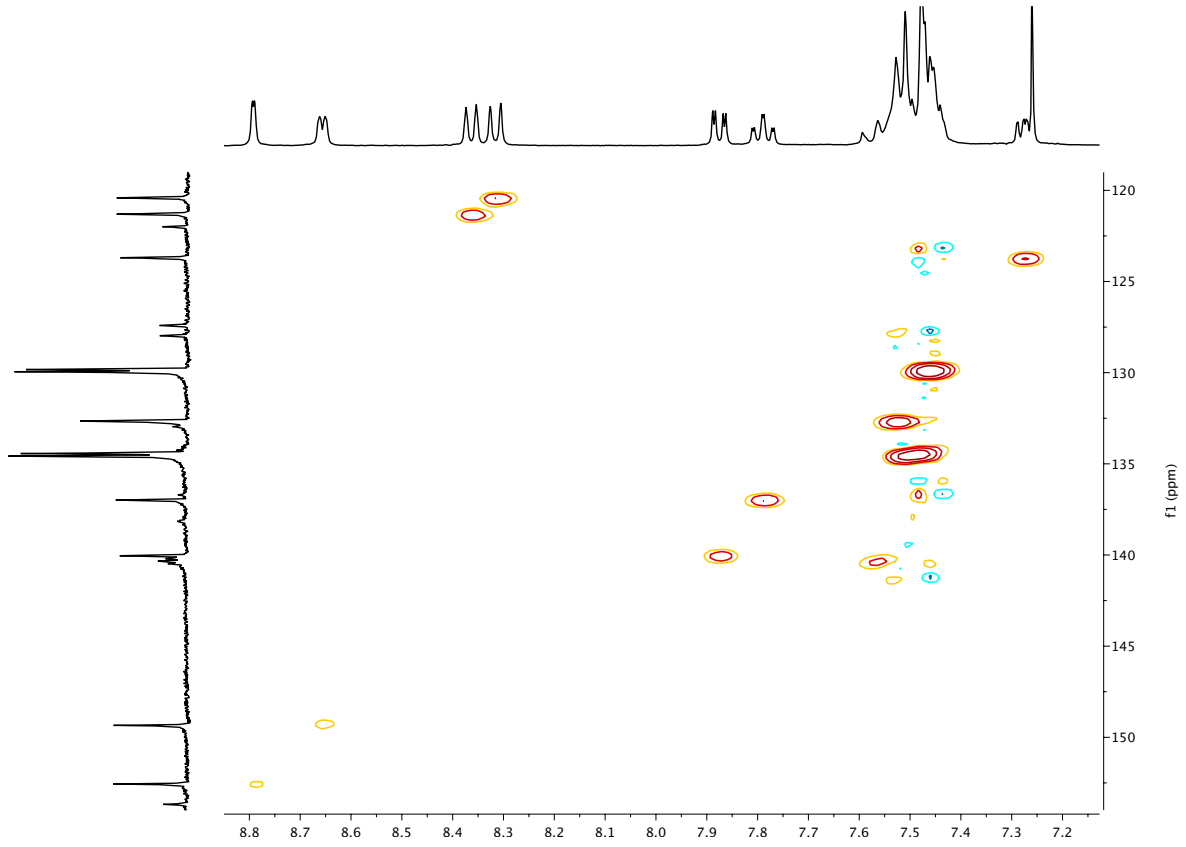


**Figure S9**. $^{1}H$-$^{13}C$ gHSQC NMR of $[Au_3(C{\equiv}CC_{10}H_7N_2)_3(\mu_3\text{-triphosph})]$ **(5)** in $CDCl_3$ at 298 K.

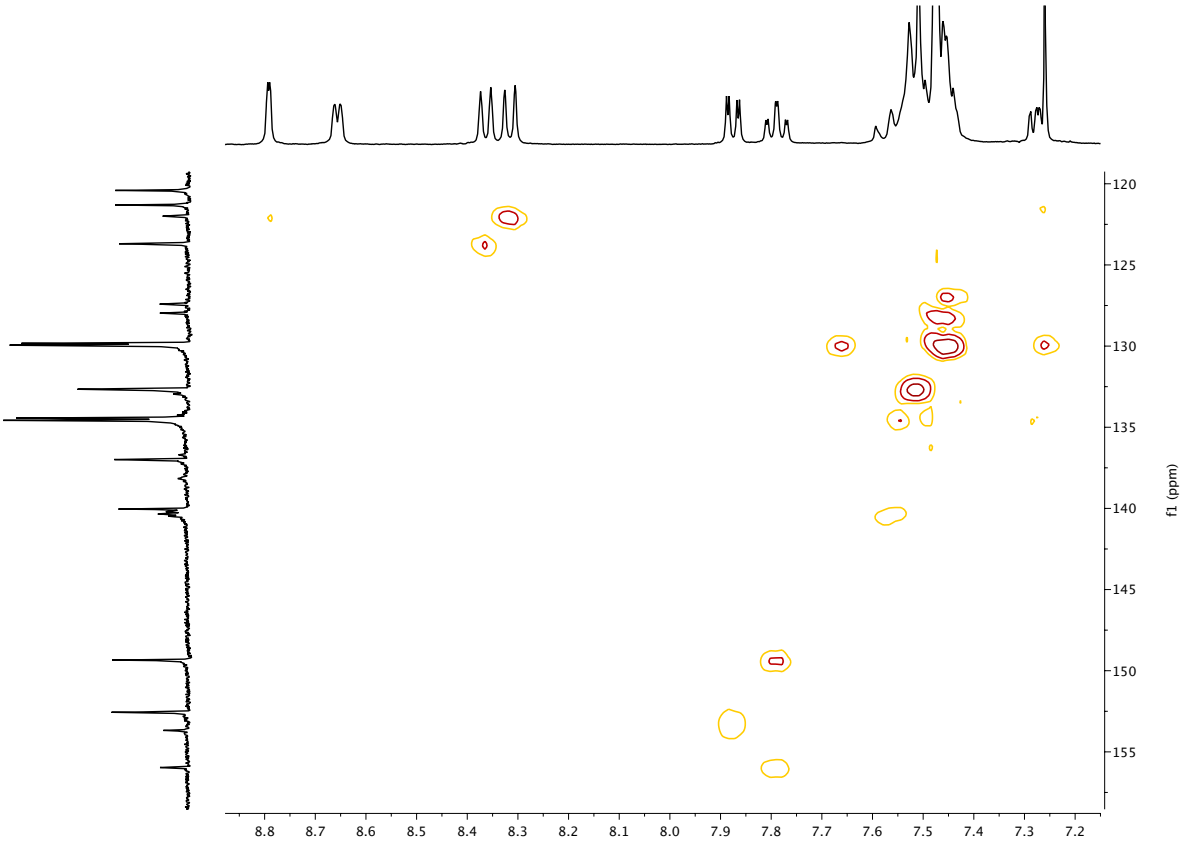


**Figure S10**. $^{1}H$-$^{13}C$ HMBC NMR of $[Au_3(C{\equiv}CC_{10}H_7N_2)_3(\mu_3\text{-triphosph})]$ **(5)** in $CDCl_3$ at 298 K.

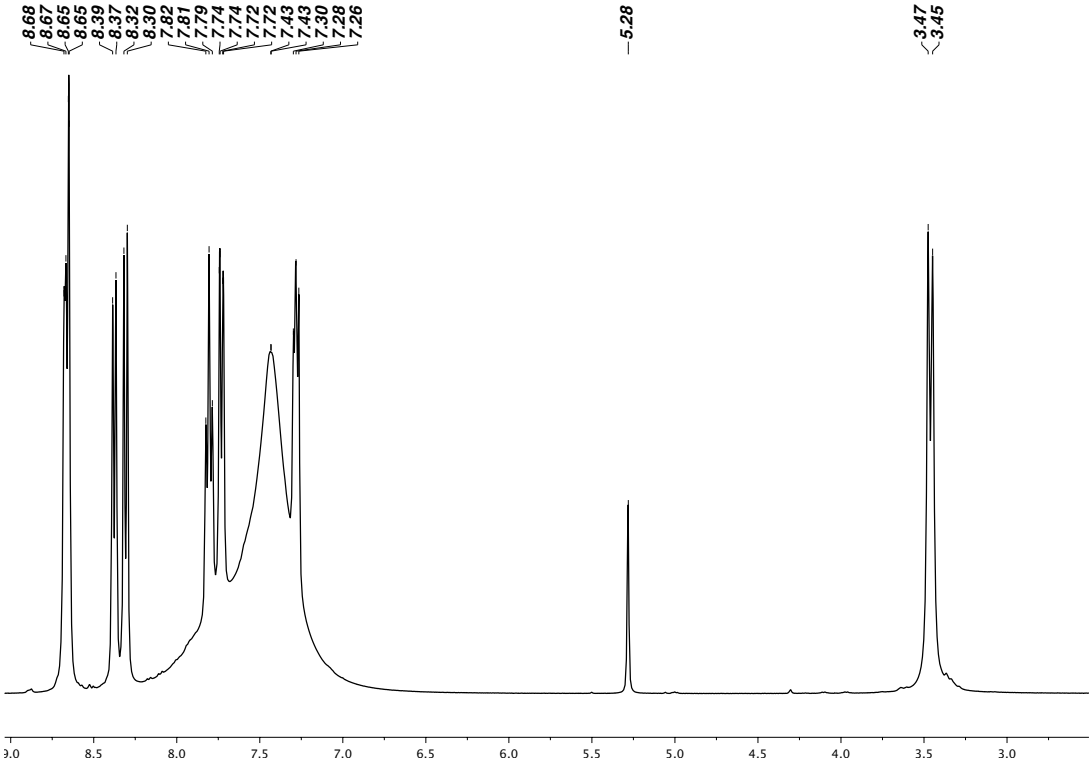


**Figure S11**. $^{1}H$ NMR of $[Au_4(C{\equiv}CC_{10}H_7N_2)_4(\mu_4\text{-tetraphos})]$ **(6)** in $CDCl_3$ at 298 K.

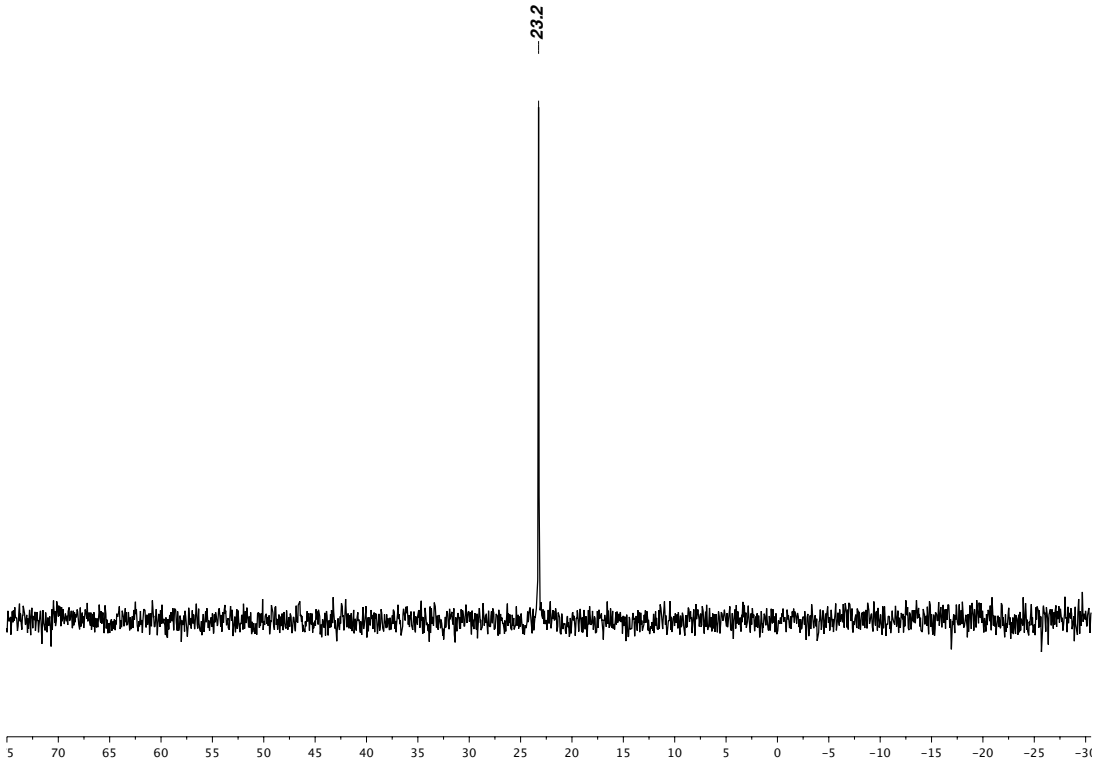


**Figure S12**. $^{31}P\{^{1}H\}$ NMR of $[Au_4(C{\equiv}CC_{10}H_7N_2)_4(\mu_4\text{-tetraphos})]$ **(6)** in $CDCl_3$ at 298 K.

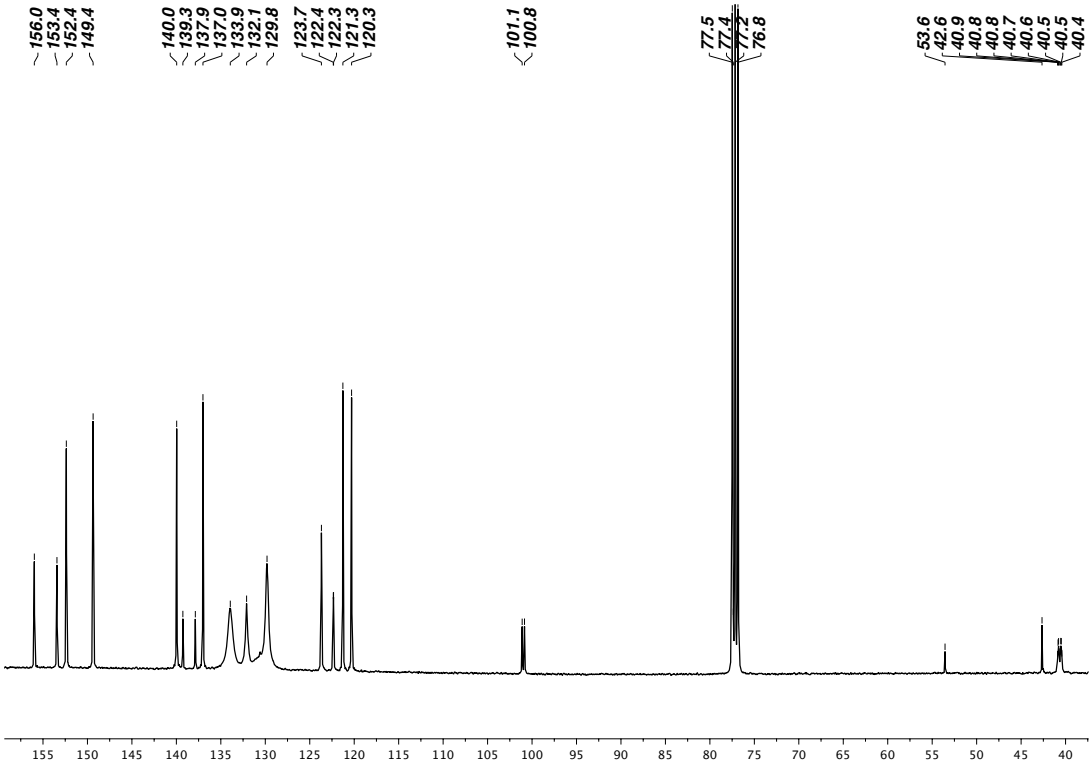


**Figure S13**. $^{13}C\{^{1}H\}$ NMR of $[Au_4(C{\equiv}CC_{10}H_7N_2)_4(\mu_4\text{-tetraphos})]$ **(6)** in $CDCl_3$ at 298 K.

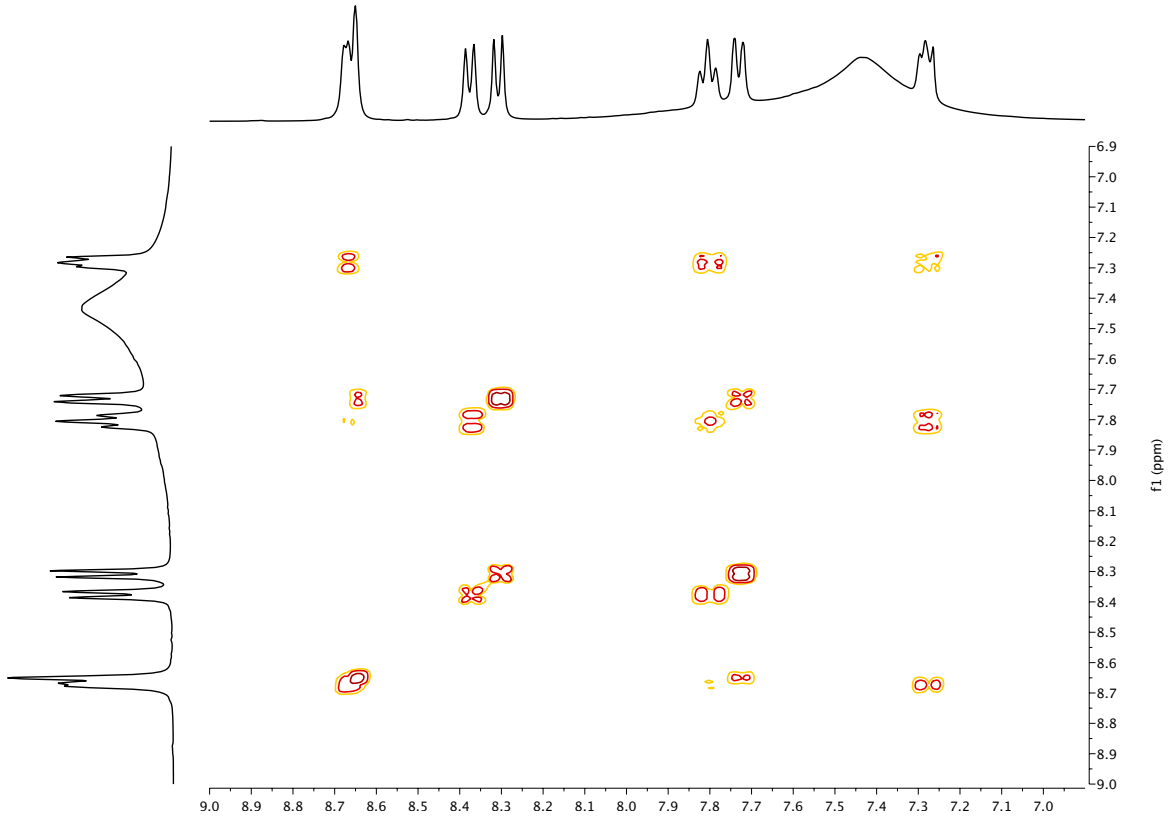


**Figure S14**. $^{1}H\text{-}^{1}H$ COSY NMR of $[Au_4(C{\equiv}CC_{10}H_7N_2)_4(\mu_4\text{-tetraphos})]$ **(6)** in $CDCl_3$ at 298 K.

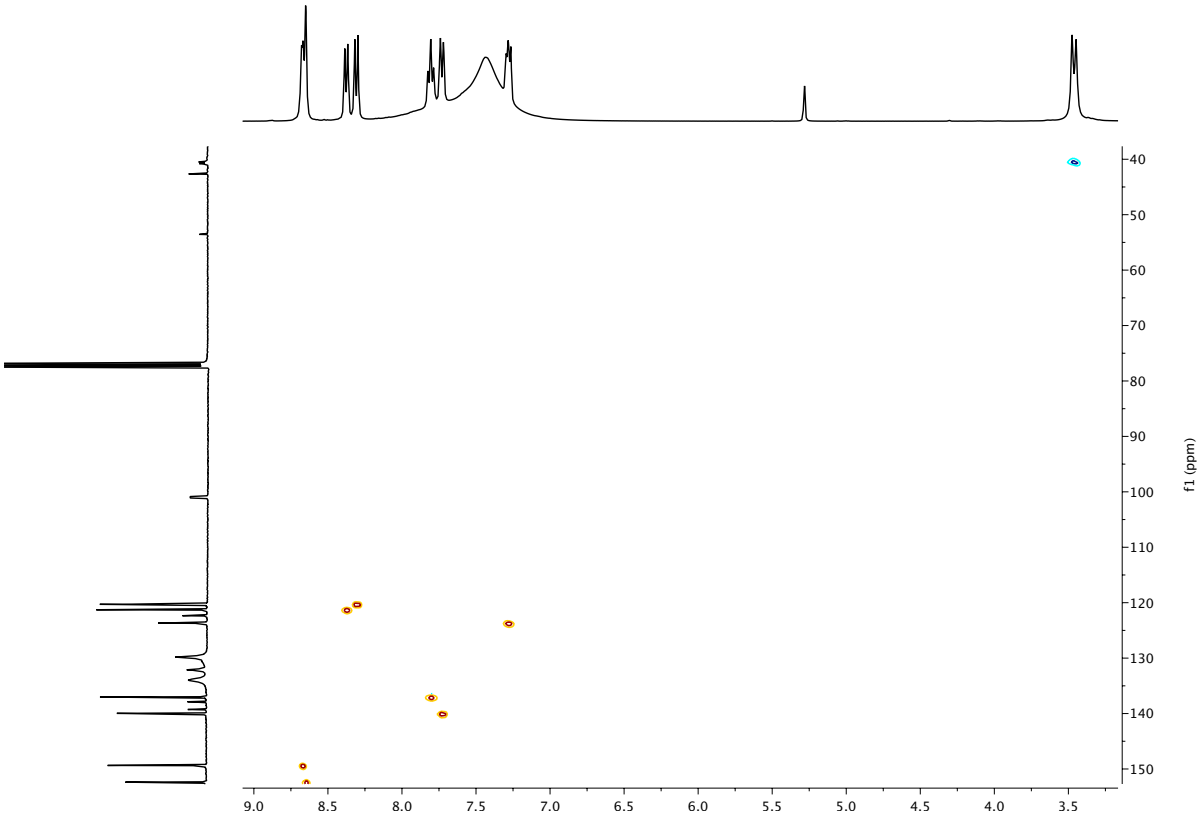


**Figure S15**. $^{1}H$-$^{13}C$ HSQC NMR of $[Au_4(C{\equiv}CC_{10}H_7N_2)_4(\mu_4\text{-tetraphos})]$ **(6)** in $CDCl_3$ at 298 K.

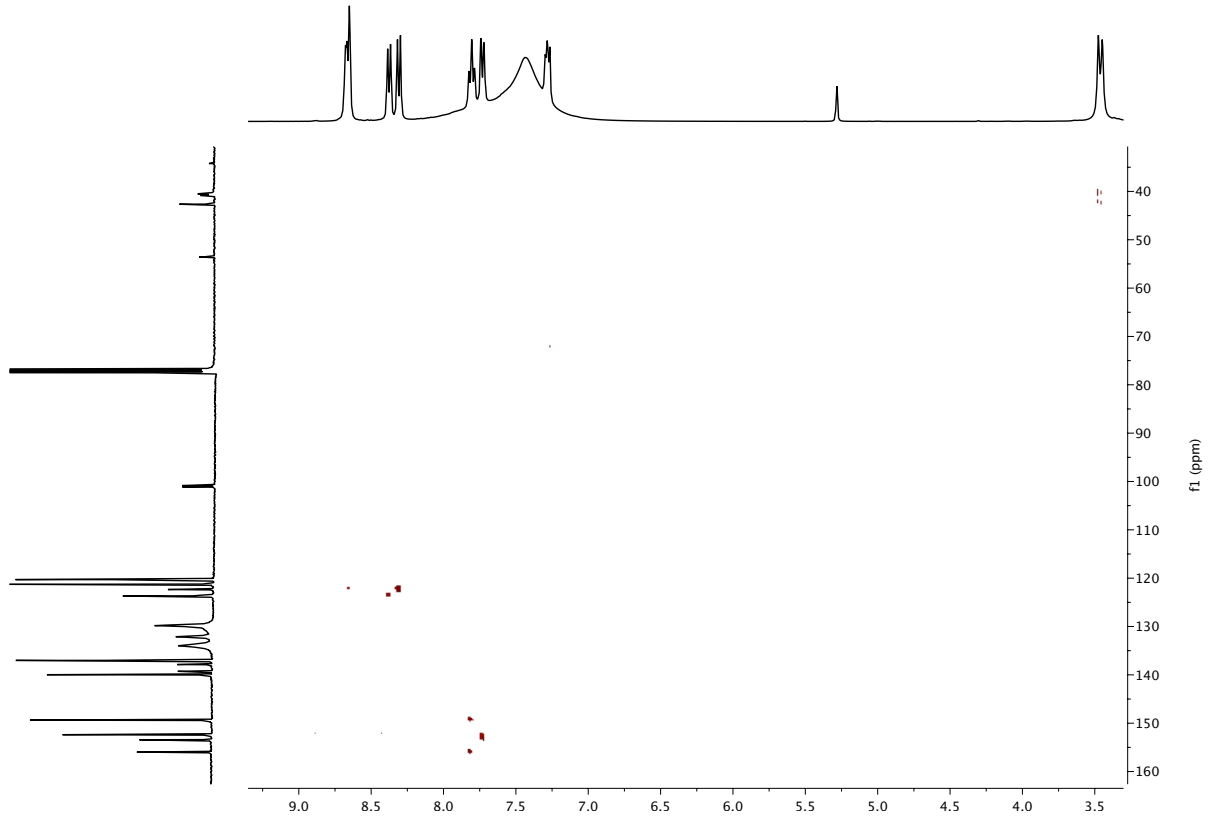


**Figure S16**. $^{1}H$-$^{13}C$ HMBC NMR of $[Au_4(C{\equiv}CC_{10}H_7N_2)_4(\mu_4\text{-tetraphos})]$ **(6)** in $CDCl_3$ at 298 K.

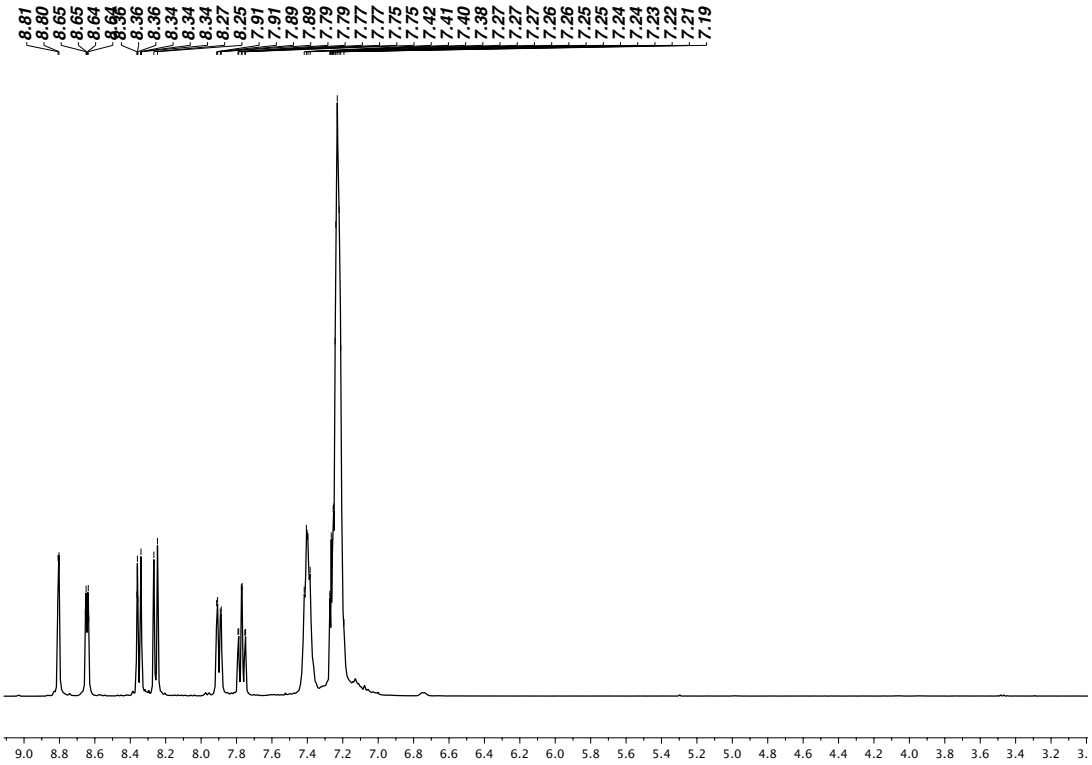


**Figure S17**. $^{1}H$ NMR of $[Au_4(C{\equiv}CC_{10}H_7N_2)_4(\mu_4\text{-tpbz})]$ **(7)** in $CDCl_3$ at 298 K.

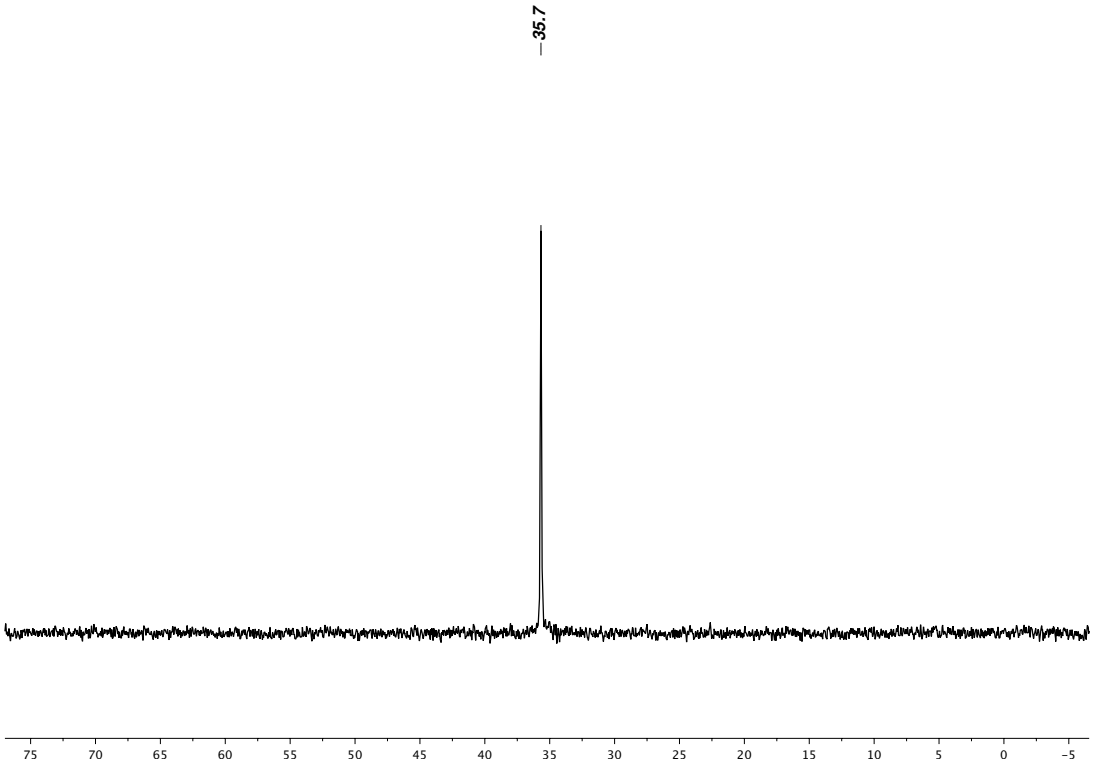


**Figure S18**. $^{31}P\{^{1}H\}$ NMR of $[Au_4(C{\equiv}CC_{10}H_7N_2)_4(\mu_4\text{-tpbz})]$ **(7)** in $CDCl_3$ at 298 K.

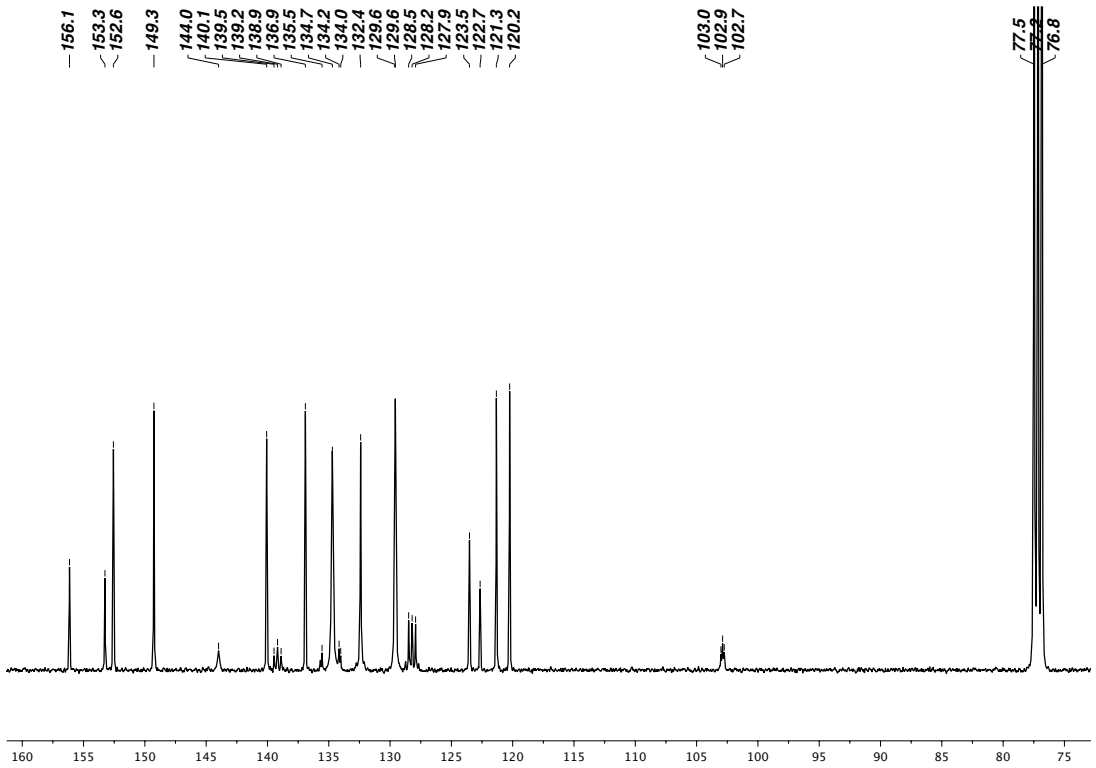


**Figure S19**. $^{13}C\{^{1}H\}$ NMR of $[Au_4(C{\equiv}CC_{10}H_7N_2)_4(\mu_4\text{-tpbz})]$ (**7**) in $CDCl_3$ at 298 K.

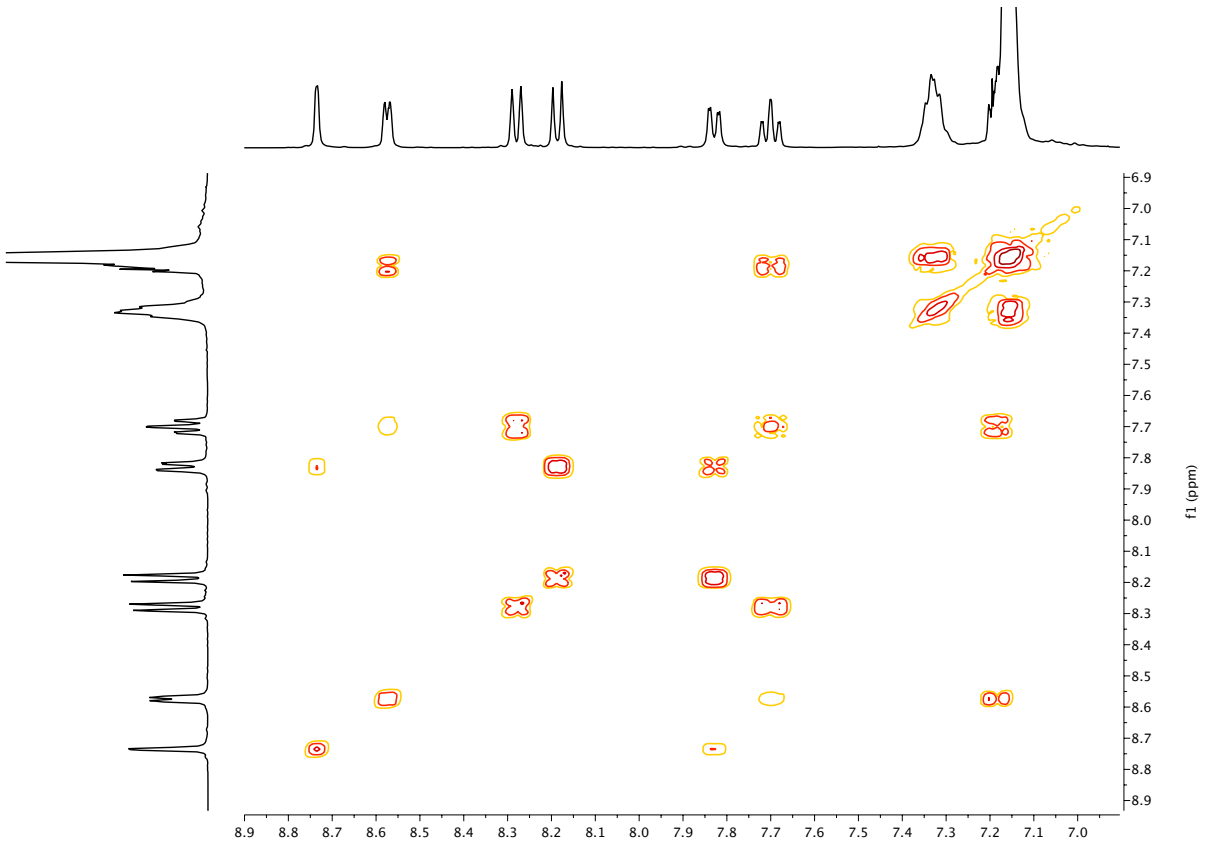


**Figure S20**. $^{1}H\text{-}^{1}H$ COSY NMR of $[Au_4(C{\equiv}CC_{10}H_7N_2)_4(\mu_4\text{-tpbz})]$ (**7**) in $CDCl_3$ at 298 K.

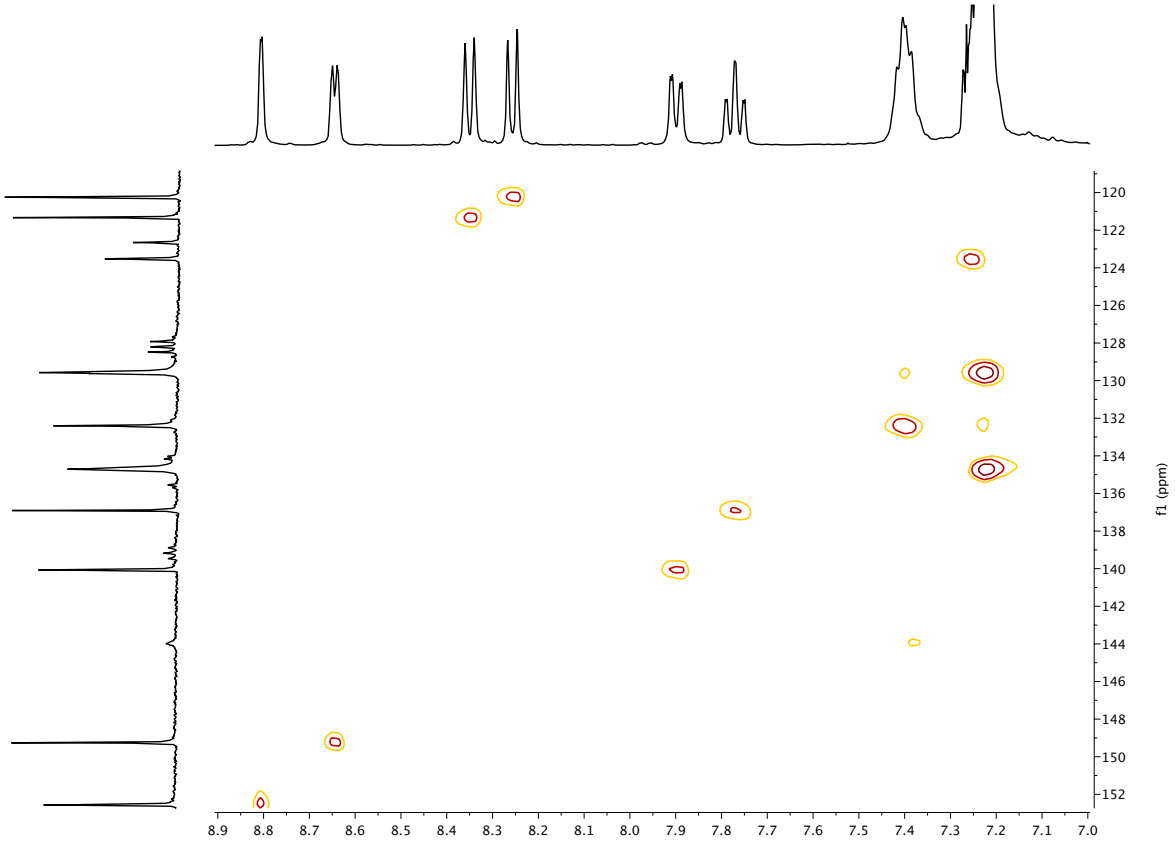


**Figure S21**. $^{1}H$-$^{31}C$ gHSQC NMR of $[Au_4(C{\equiv}CC_{10}H_7N_2)_4(\mu_4\text{-tpbz})]$ **(7)** in $CDCl_3$ at 298 K

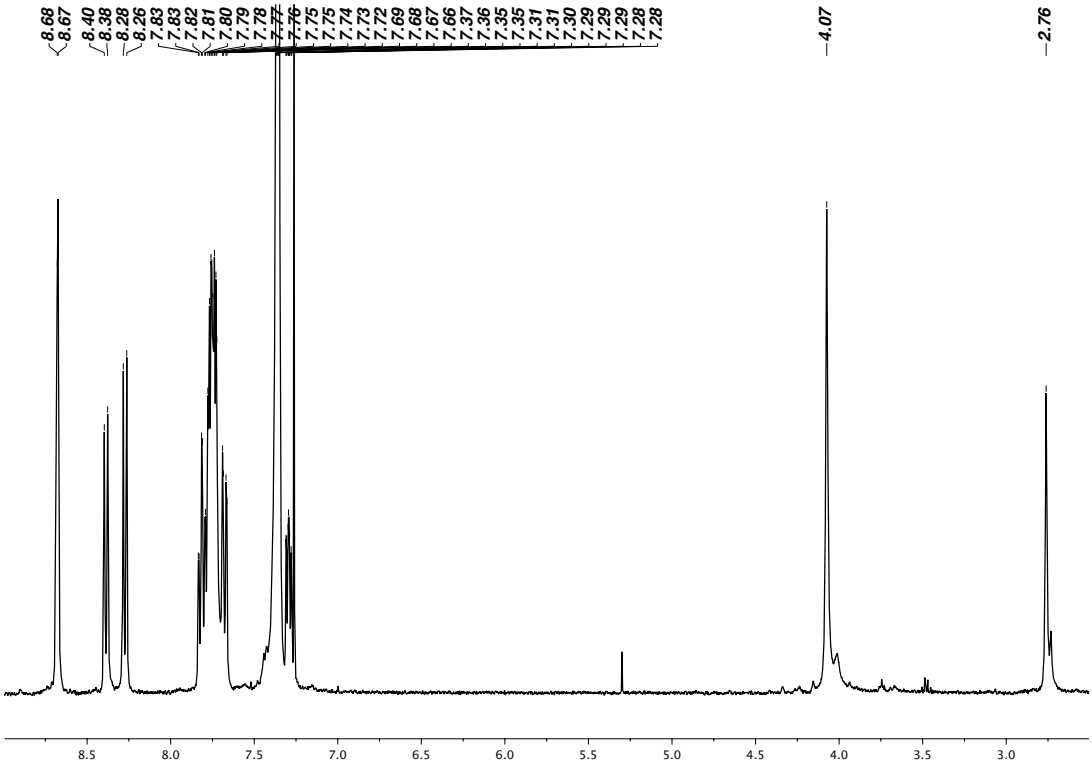


**Figure S22**. $^{1}H$ NMR of $[Au_4(C{\equiv}CC_{10}H_7N_2)_4(\mu_4\text{-dppeda})]$ **(8)** in $CDCl_3$ at 298 K.

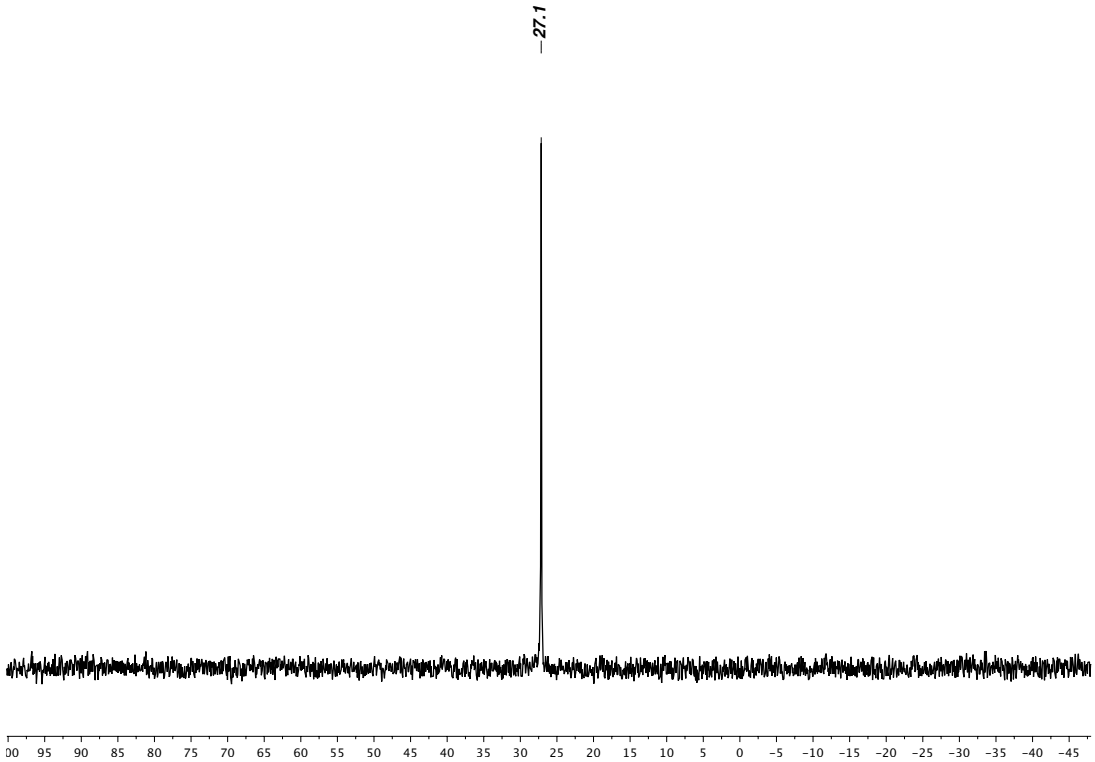


**Figure S23**. $^{31}P\{^{1}H\}$ NMR of $[Au_4(C{\equiv}CC_{10}H_7N_2)_4(\mu_4\text{-dppeda})]$ **(8)** in $CDCl_3$ at 298 K.

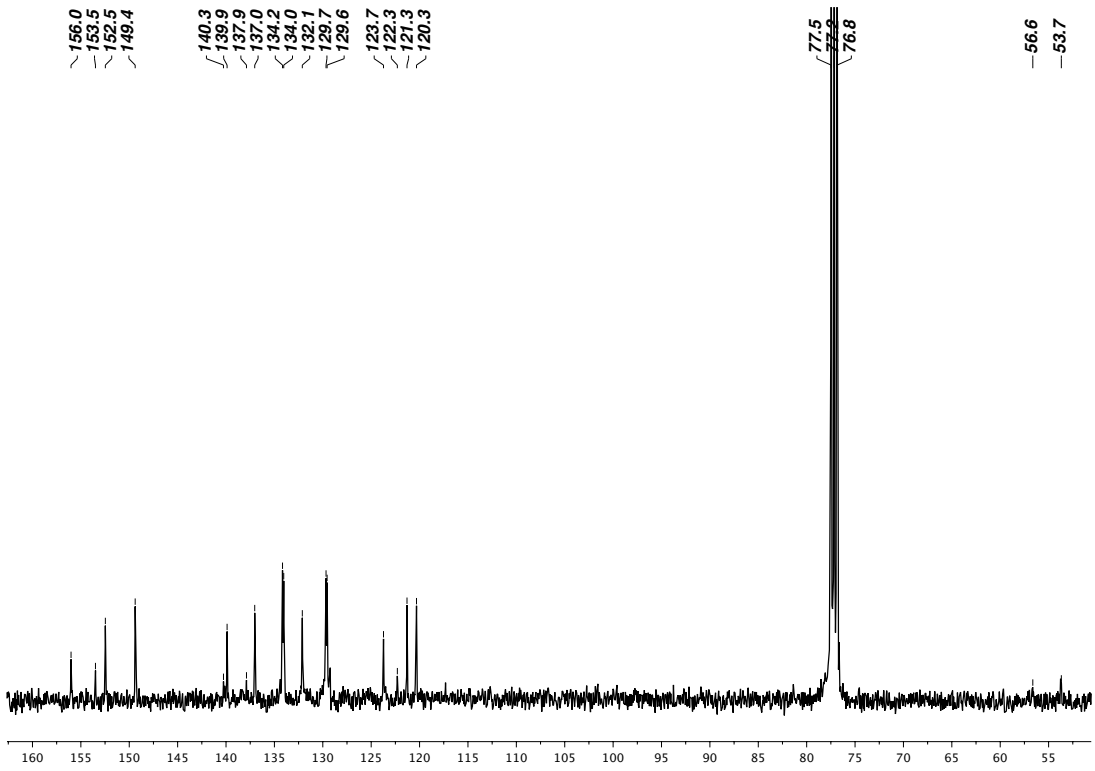


**Figure S24**. $^{13}C\{^{1}H\}$ NMR of $[Au_4(C{\equiv}CC_{10}H_7N_2)_4(\mu_4\text{-dppeda})]$ **(8)** in $CDCl_3$ at 298 K.

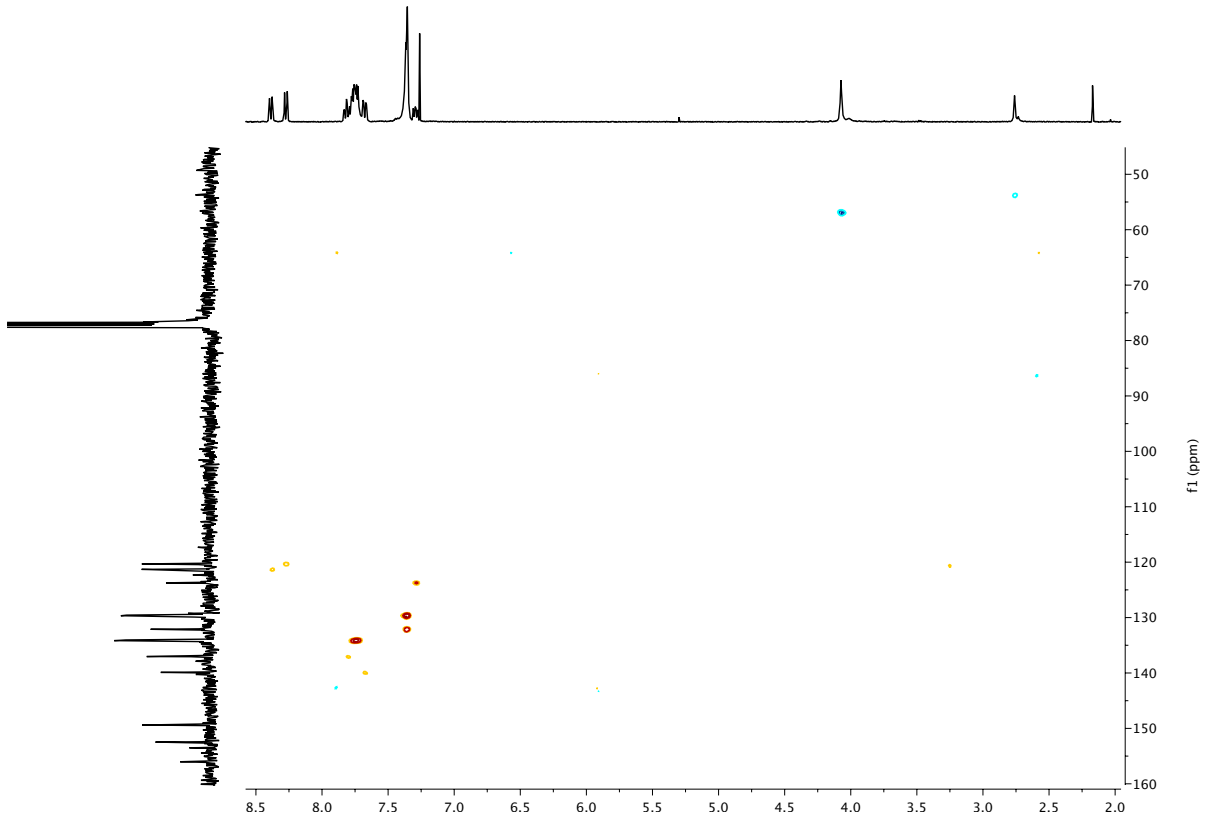


**Figure S25**. $^{1}H$-$^{13}C$ gHSQC NMR of $[Au_4(C{\equiv}CC_{10}H_7N_2)_4(\mu_4\text{-dppeda})]$ **(8)** in $CDCl_3$ at 298 K.

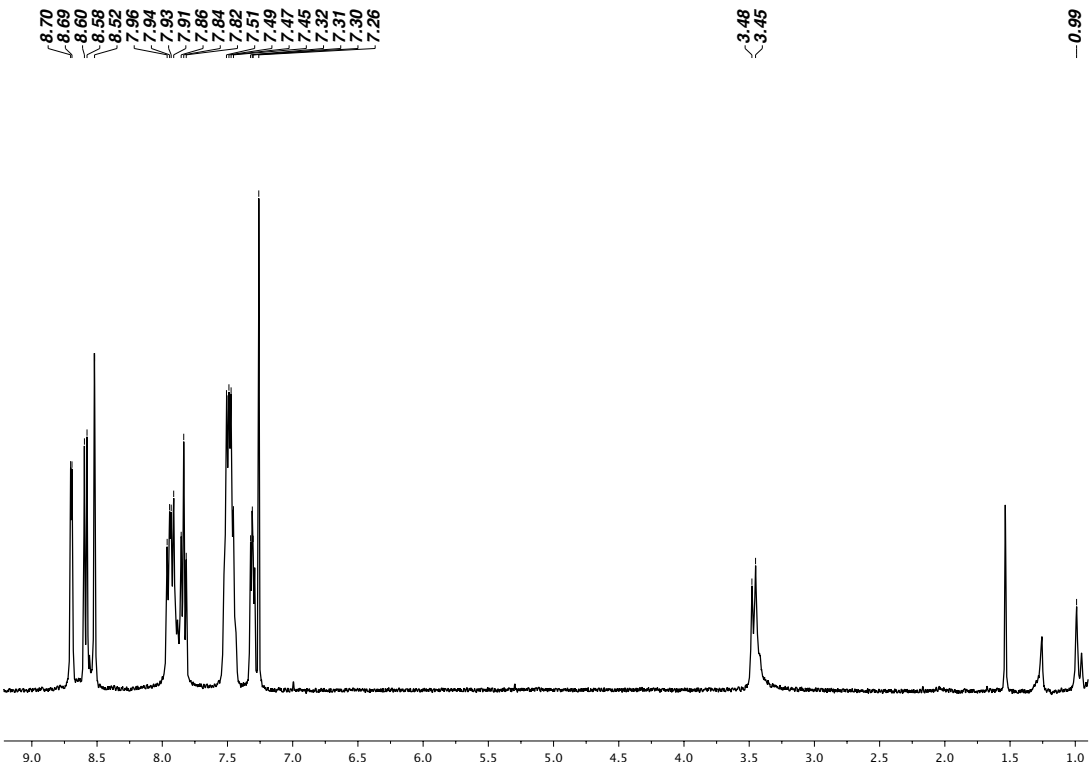


**Figure S26**. $^{1}H$ NMR of $[Au_3(C{\equiv}CC_{15}H_{10}N_3)_3(\mu_3\text{-triphos})]$ **(9)** in $CDCl_3$ at 298 K.

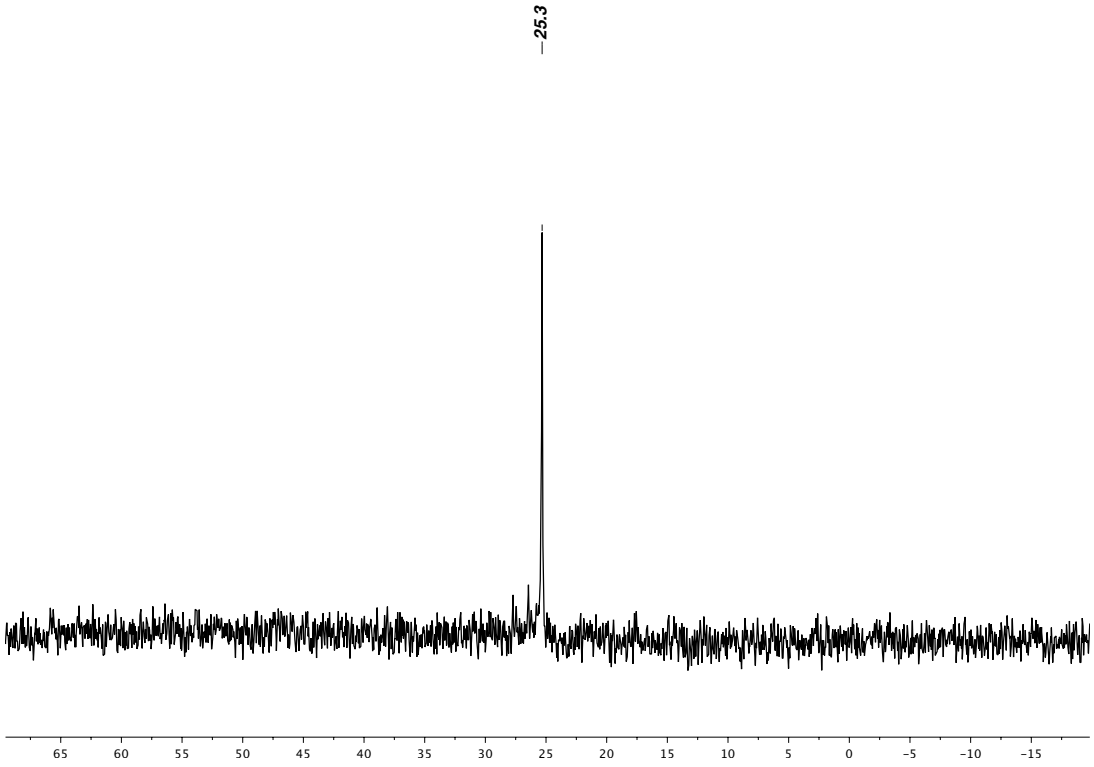


**Figure S27**. $^{31}P\{^{1}H\}$ NMR of $[Au_3(C{\equiv}CC_{15}H_{10}N_3)_3(\mu_3\text{-triphos})]$ **(9)** in $CDCl_3$ at 298 K.

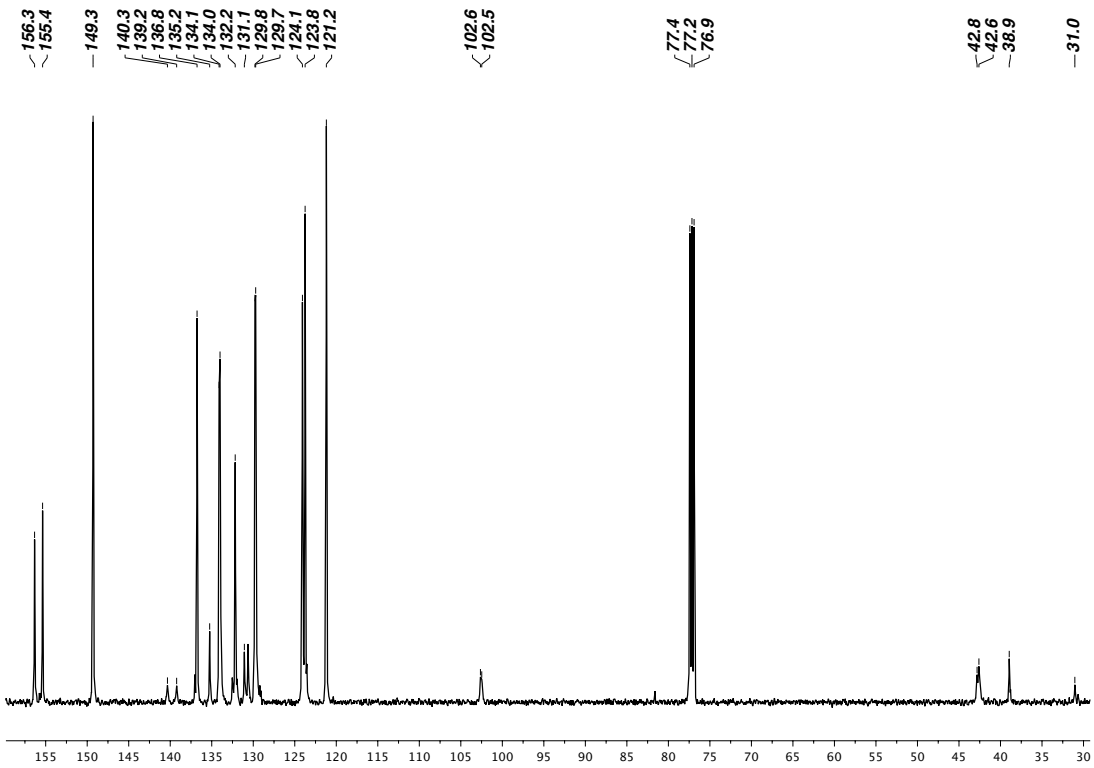


**Figure S28**. $^{13}C\{^{1}H\}$ NMR of $[Au_3(C{\equiv}CC_{15}H_{10}N_3)_3(\mu_3\text{-triphos})]$ **(9)** in $CDCl_3$ at 298 K.

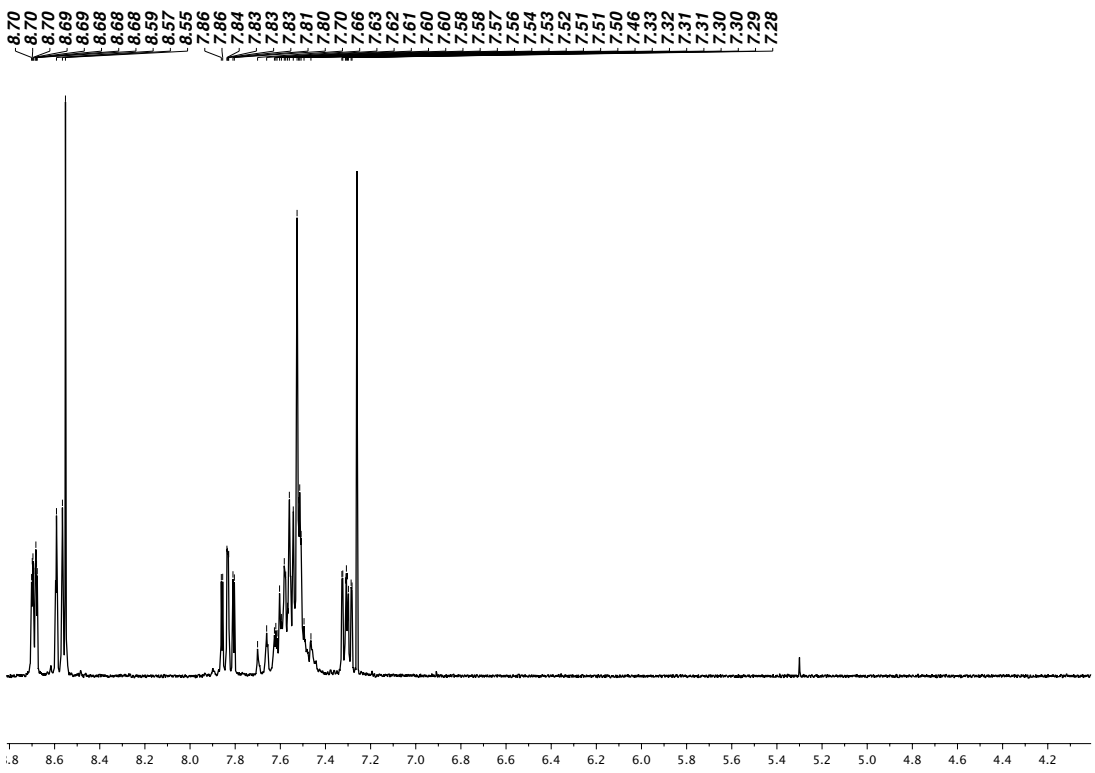


**Figure S29**. $^{1}H$ NMR of $[Au_3(C{\equiv}CC_{15}H_{10}N_3)_3(\mu_3\text{-triphosph})]$ **(10)** in $CDCl_3$ at 298 K.

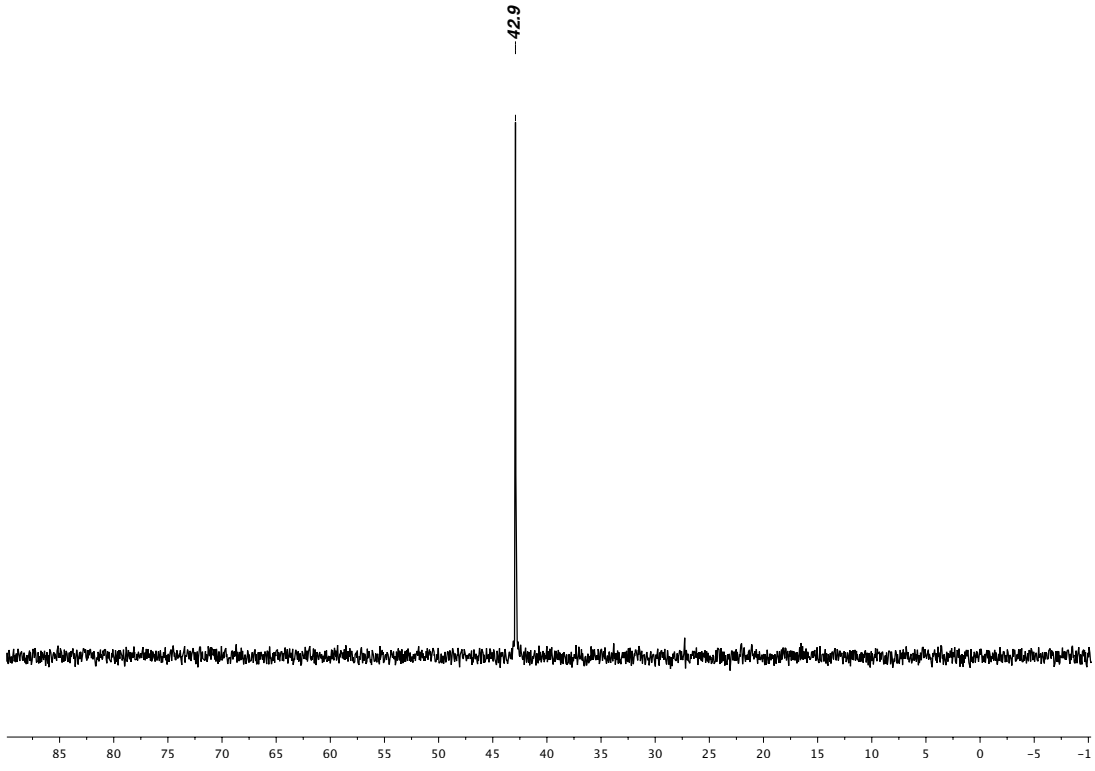


**Figure S30**. $^{31}P\{^{1}H\}$ NMR of $[Au_3(C{\equiv}CC_{15}H_{10}N_3)_3(\mu_3\text{-triphosph})]$ **(10)** in $CDCl_3$ at 298 K.

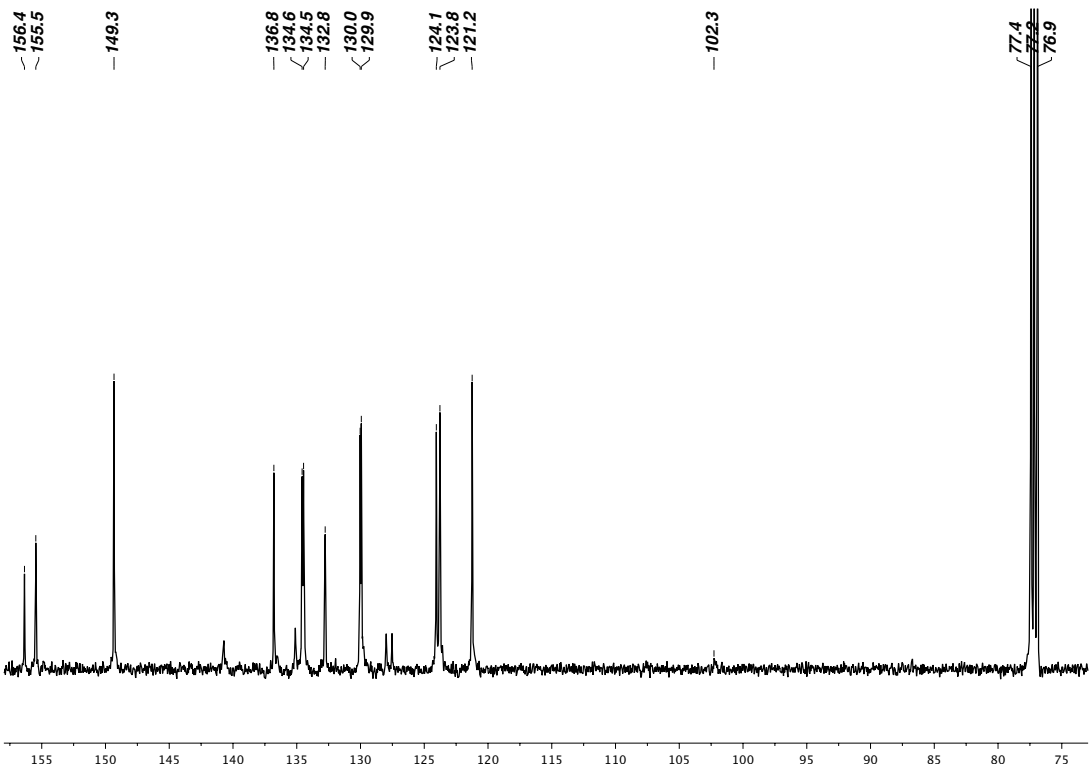


**Figure S31**. $^{13}C\{^{1}H\}$ NMR of $[Au_3(C{\equiv}CC_{15}H_{10}N_3)_3(\mu_3\text{-triphosph})]$ **(10)** in $CDCl_3$ at 298 K.

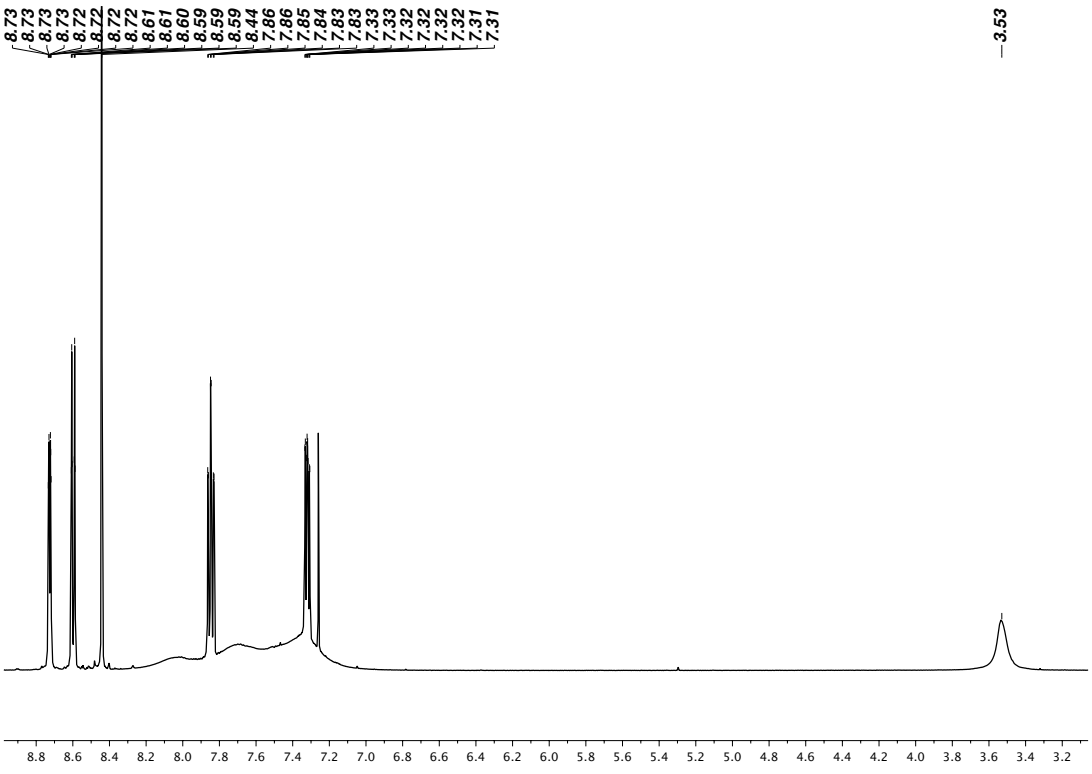


**Figure S32**. $^{1}H$ NMR of $[Au_4(C{\equiv}CC_{15}H_{10}N_3)_4(\mu_4\text{-tetraphos})]$ **(11)** in $CDCl_3$ at 298 K.

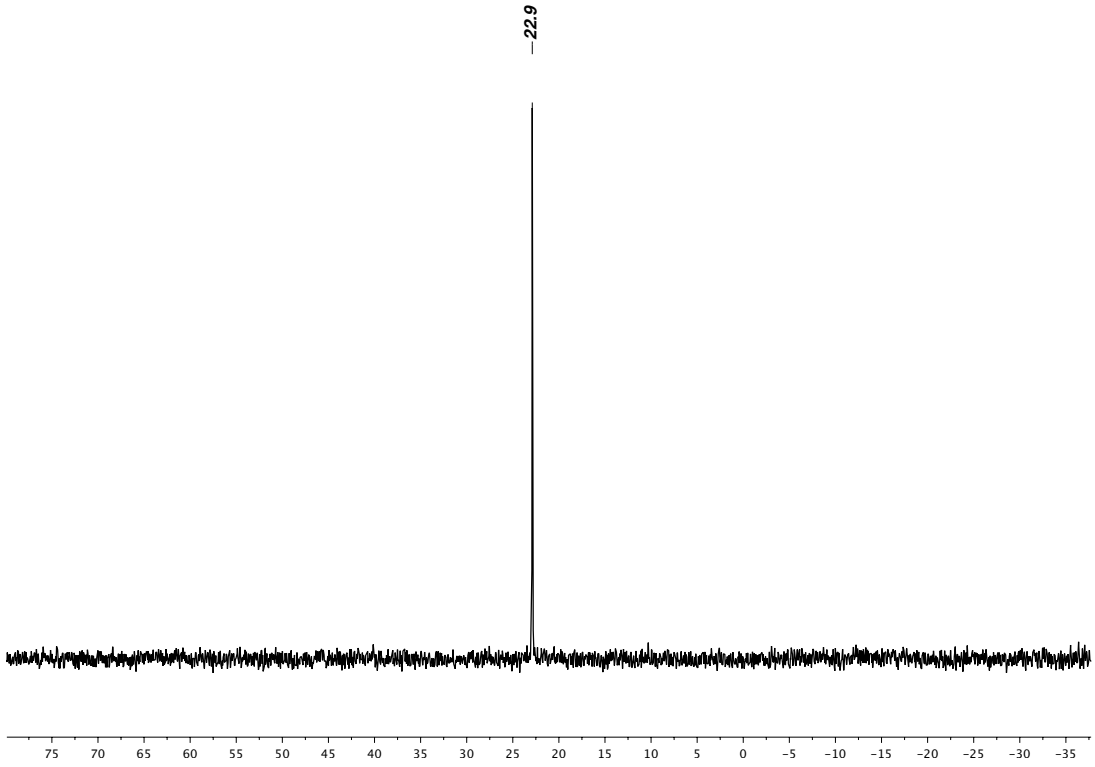


**Figure S33**. $^{31}P\{^{1}H\}$ NMR of $[Au_4(C{\equiv}CC_{15}H_{10}N_3)_4(\mu_4\text{-tetraphos})]$ **(11)** in $CDCl_3$ at 298 K.

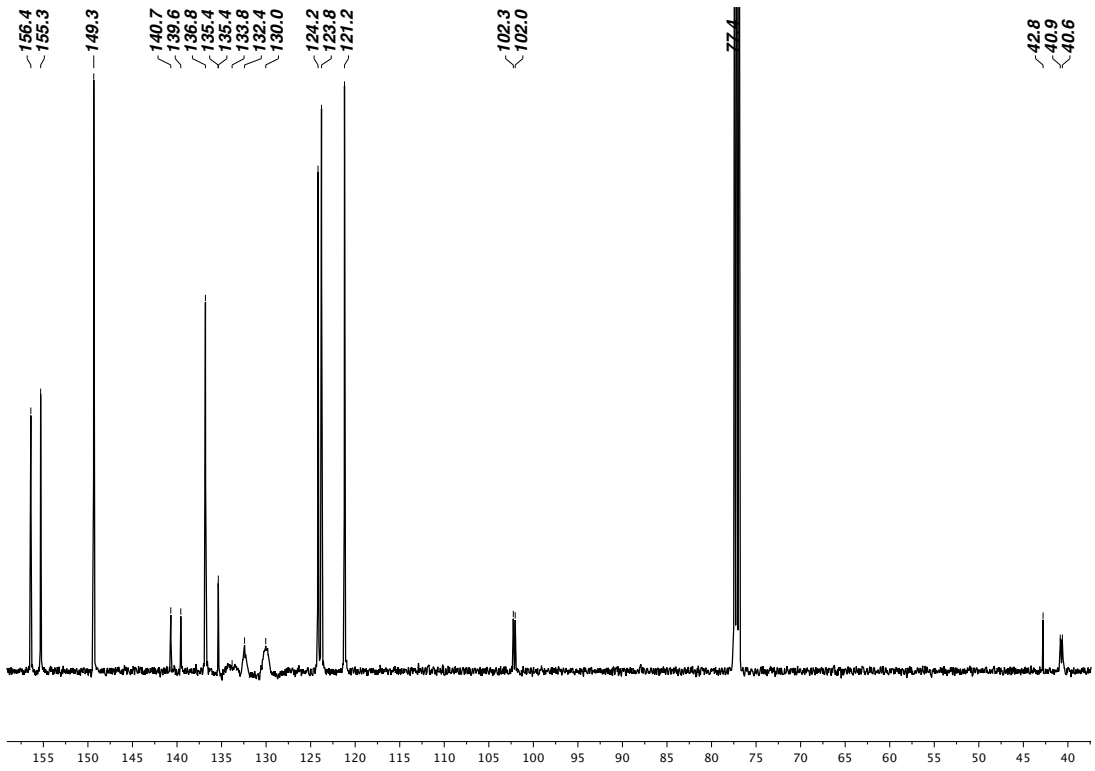


**Figure S34**. $^{13}C\{^{1}H\}$ NMR of $[Au_4(C{\equiv}CC_{15}H_{10}N_3)_4(\mu_4\text{-tetraphos})]$ **(11)** in $CDCl_3$ at 298 K.

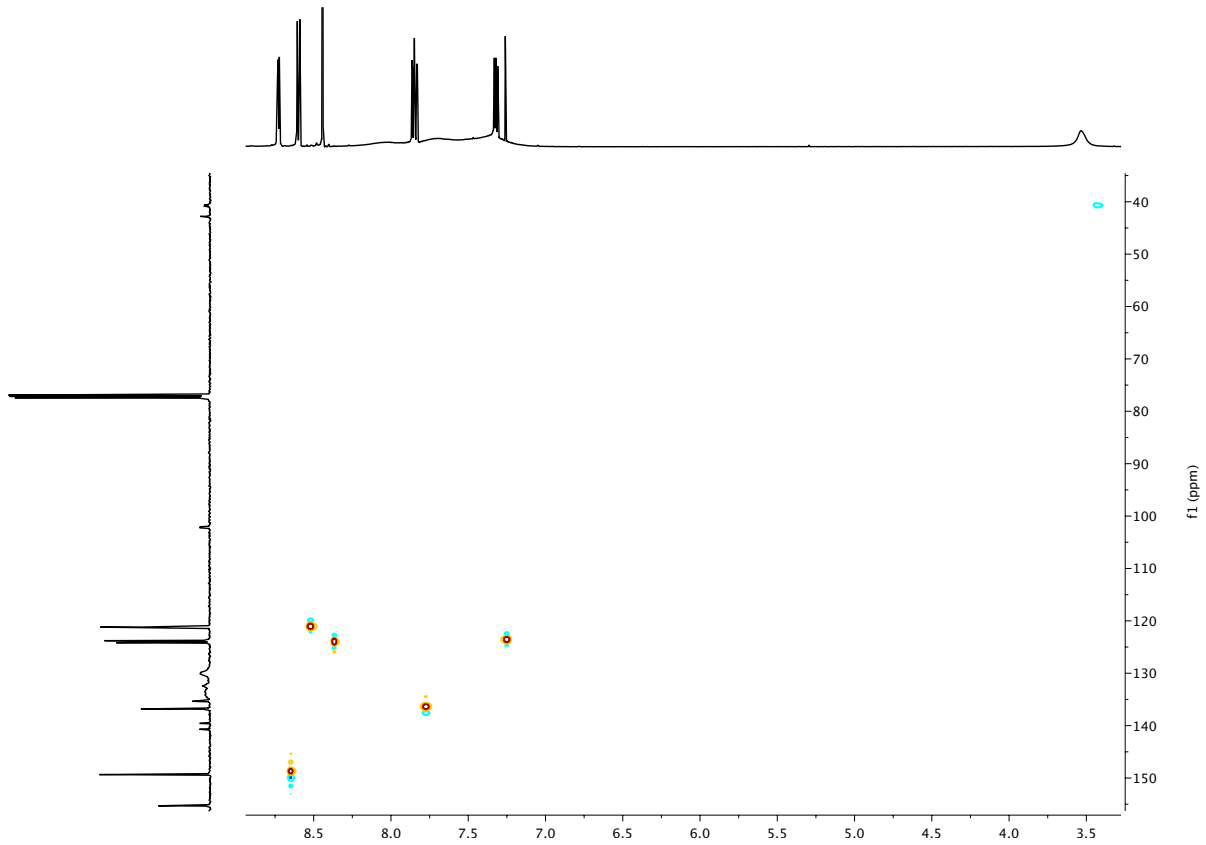


**Figure S35**. $^{1}H$-$^{13}C$ HSQC NMR of $[Au_4(C{\equiv}CC_{15}H_{10}N_3)_4(\mu_4\text{-tetraphos})]$ **(11)** in $CDCl_3$ at 298 K.

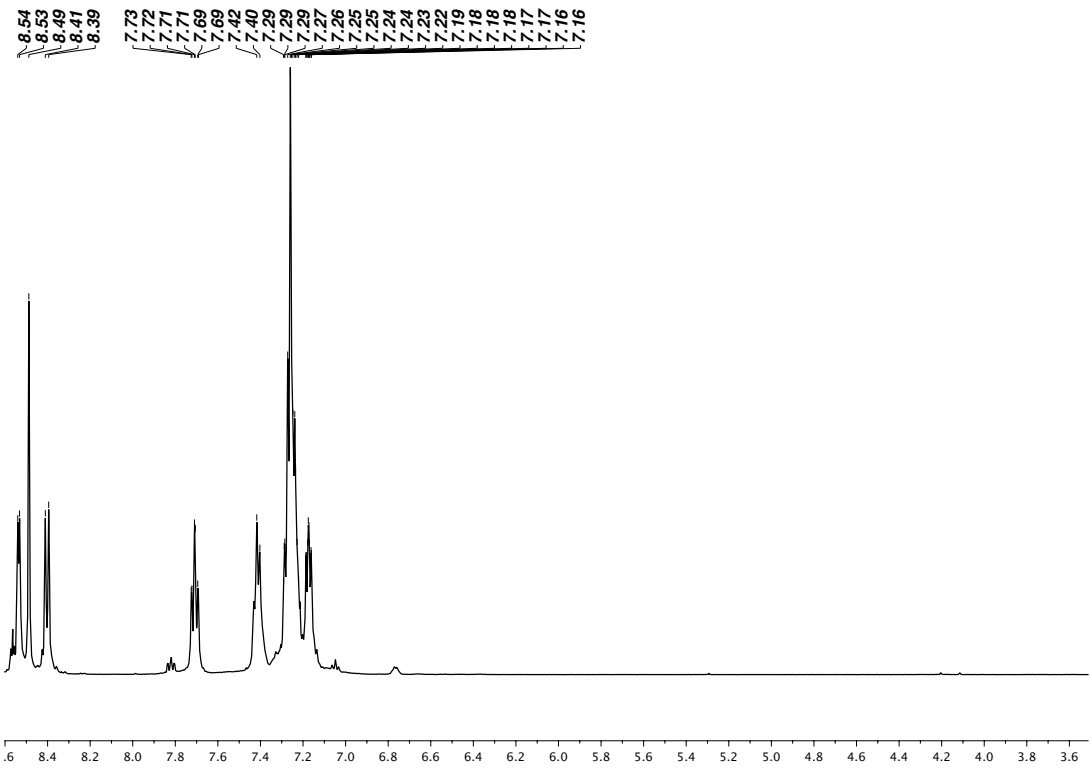


**Figure S36**. $^{1}H$ NMR of $[Au_4(C{\equiv}CC_{15}H_{10}N_3)_4(\mu_4\text{-tpbz})]$ **(12)** in $CDCl_3$ at 298 K.

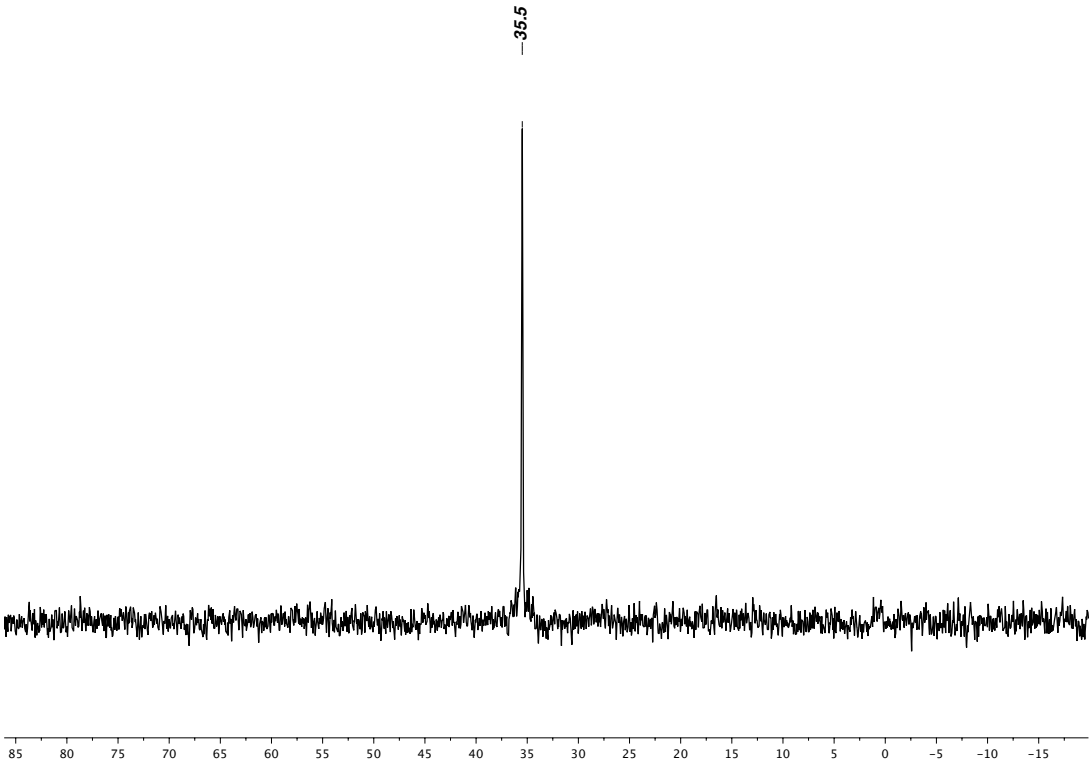


**Figure S37**. $^{31}P\{^{1}H\}$ NMR of $[Au_4(C{\equiv}CC_{15}H_{10}N_3)_4(\mu_4\text{-tpbz})]$ **(12)** in $CDCl_3$ at 298 K.

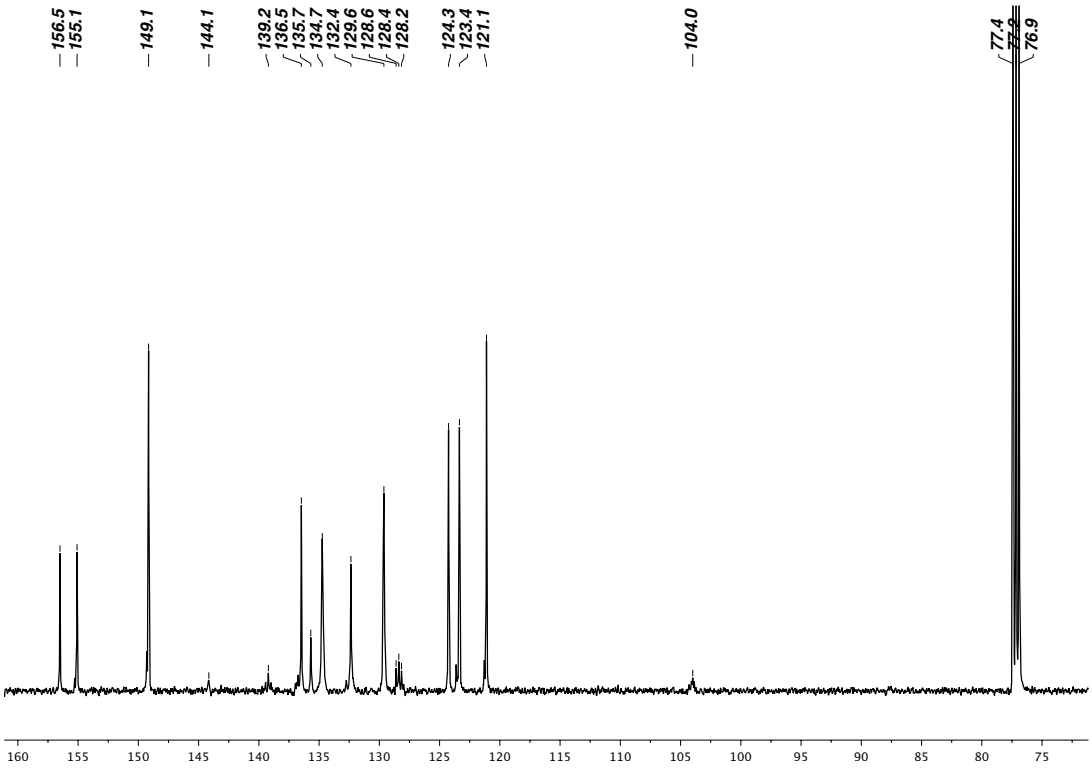


**Figure S38**. $^{13}C\{^{1}H\}$ NMR of $[Au_4(C{\equiv}CC_{15}H_{10}N_3)_4(\mu_4\text{-tpbz})]$ **(12)** in $CDCl_3$ at 298 K.

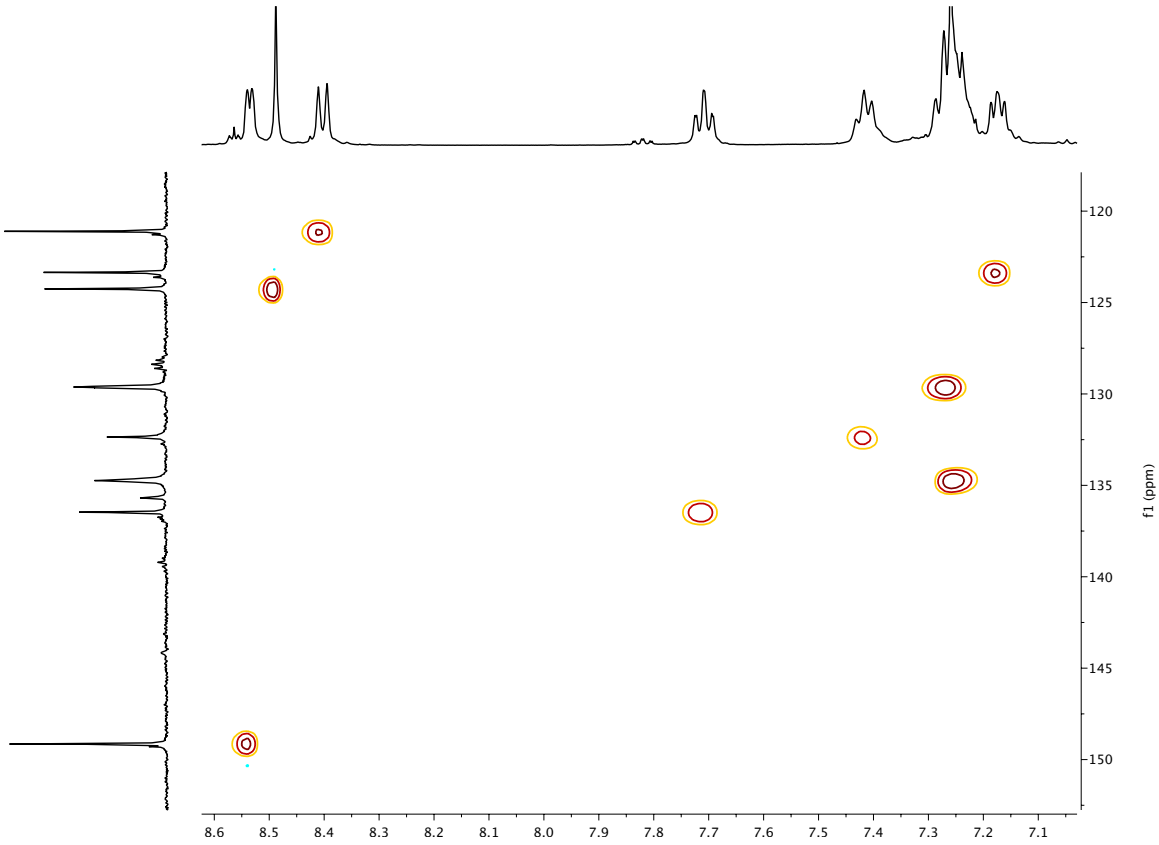


**Figure S39**. $^{1}H$-$^{13}C$ gHSQC NMR of $[Au_4(C{\equiv}CC_{15}H_{10}N_3)_4(\mu_4\text{-tpbz})]$ **(12)** in $CDCl_3$ at 298 K.

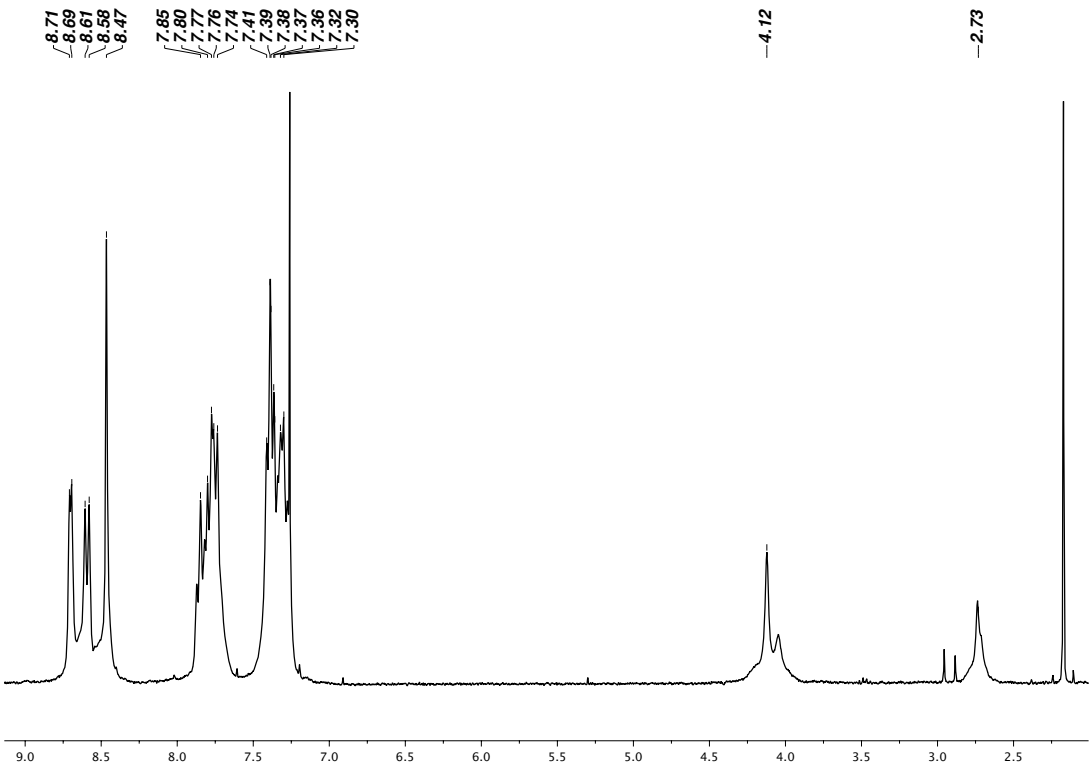


**Figure S40**. $^{1}H$ NMR of $[Au_4(C{\equiv}CC_{15}H_{10}N_3)_4(\mu_4\text{-dppeda})]$ **(13)** in $CDCl_3$ at 298 K.

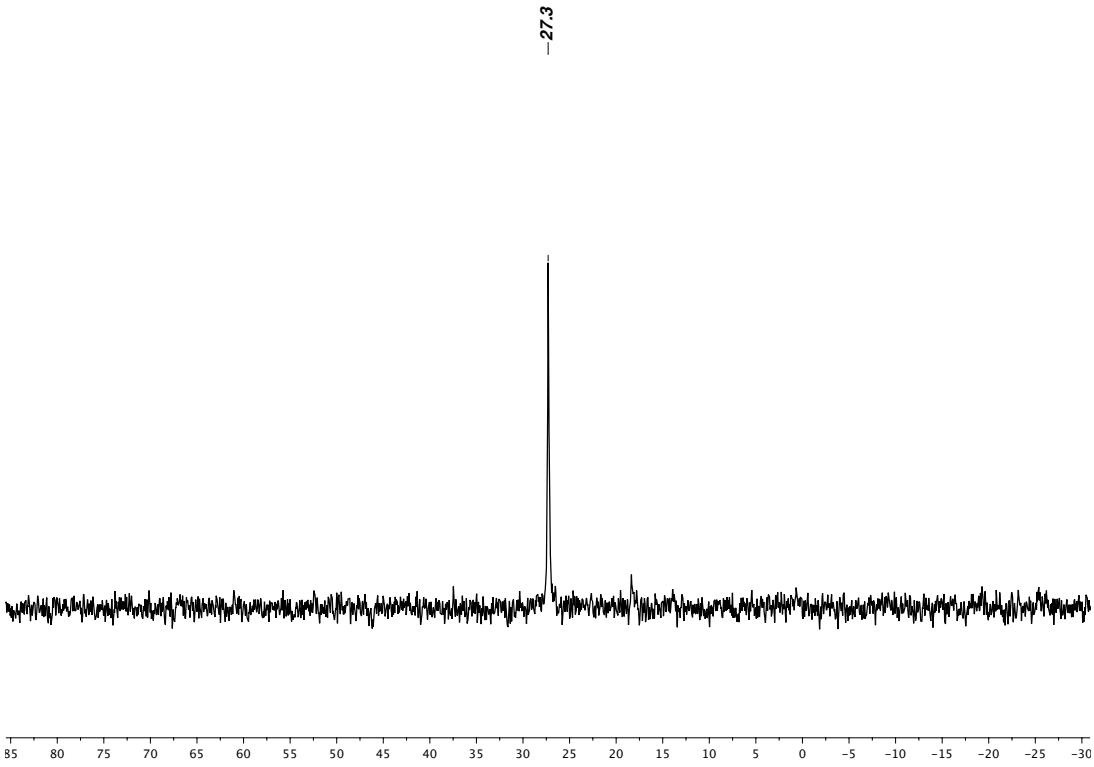


**Figure S41**. $^{31}P\{^{1}H\}$ NMR of $[Au_4(C{\equiv}CC_{15}H_{10}N_3)_4(\mu_4\text{-dppeda})]$ **(13)** in $CDCl_3$ at 298 K.

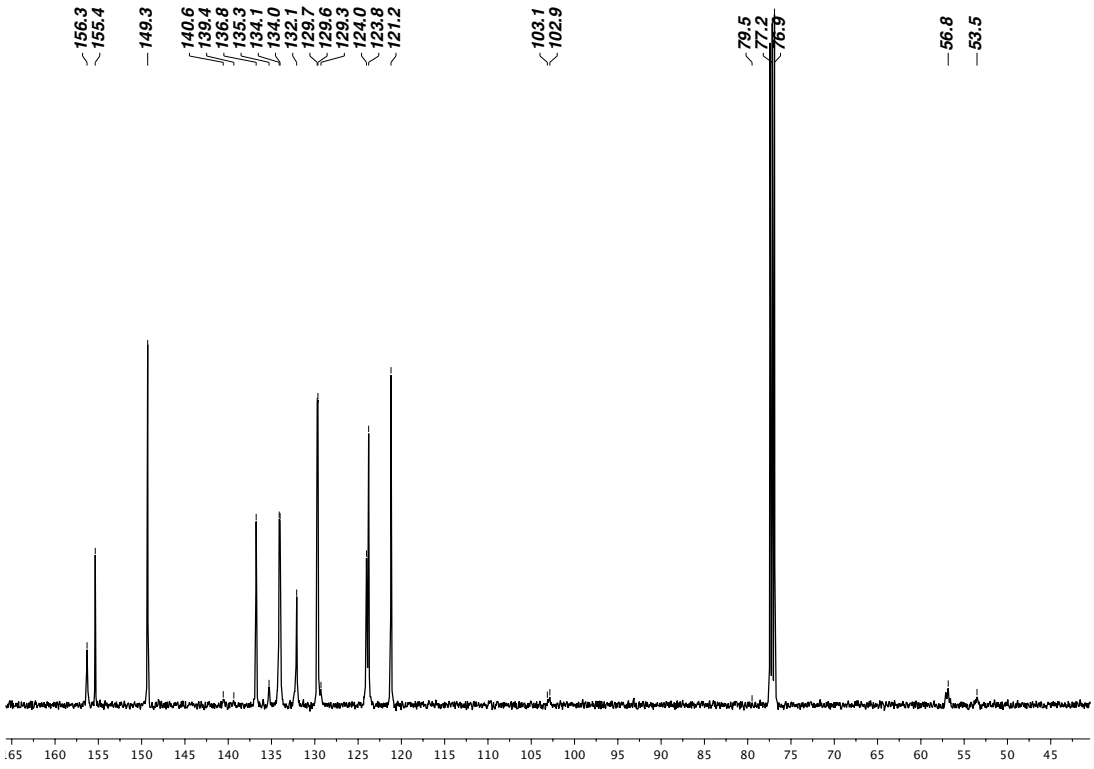


**Figure S42**. $^{13}C$ NMR of $[Au_4(C{\equiv}CC_{15}H_{10}N_3)_4(\mu_4\text{-dppeda})]$ **(13)** in $CDCl_3$ at 298 K.

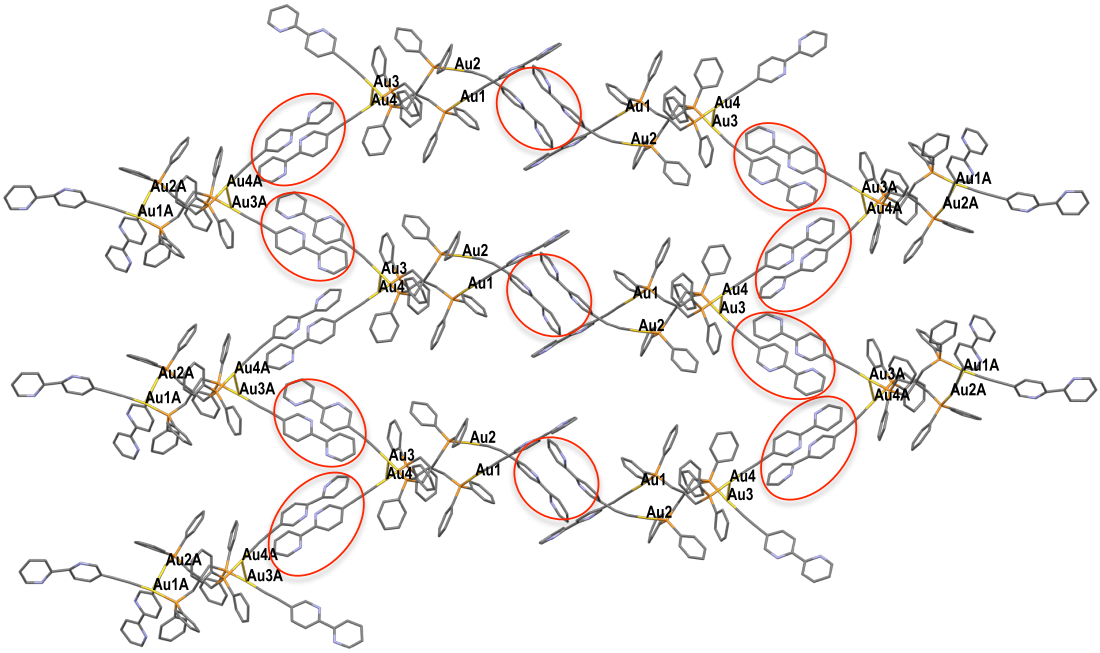


**Figure S43.** View of the molecular packing of compound **6**. π-π interactions between bipyridine rings of different molecules are highlighted in red.

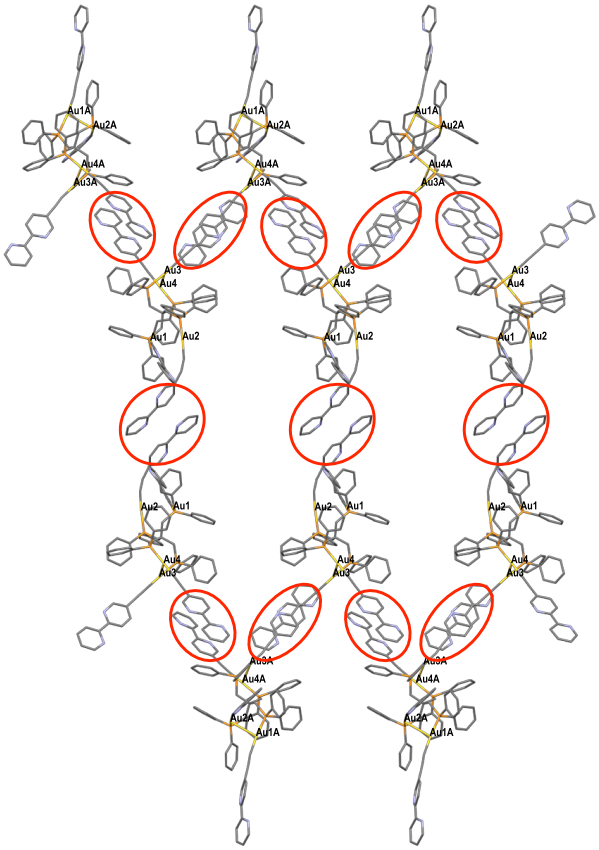

**Figure S44.** View of the molecular packing of compound **6** following the crystallographic a* axis. π-π interactions between bipyridine rings of different molecules are highlighted in red.

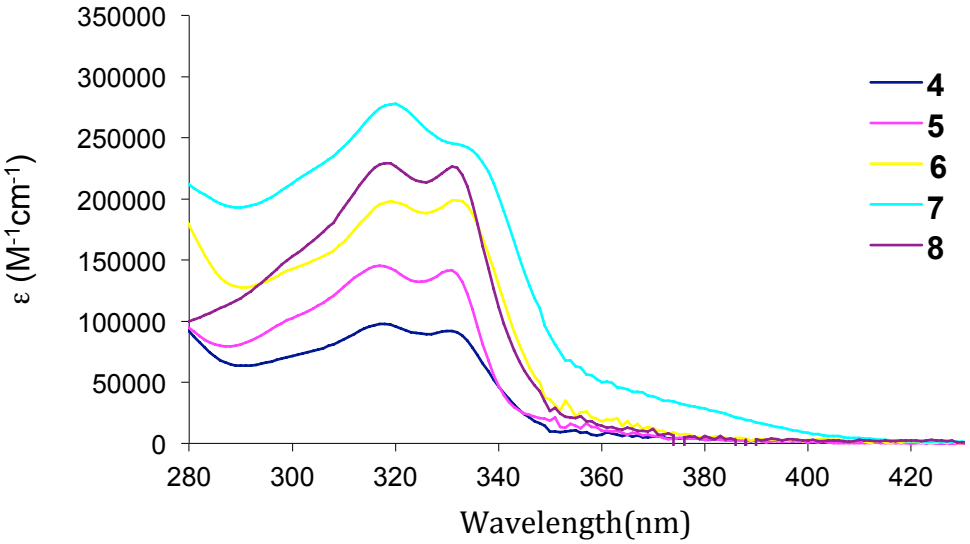


**Figure S45.** Absorption spectra of dichloromethane solutions of compounds **4-8**.

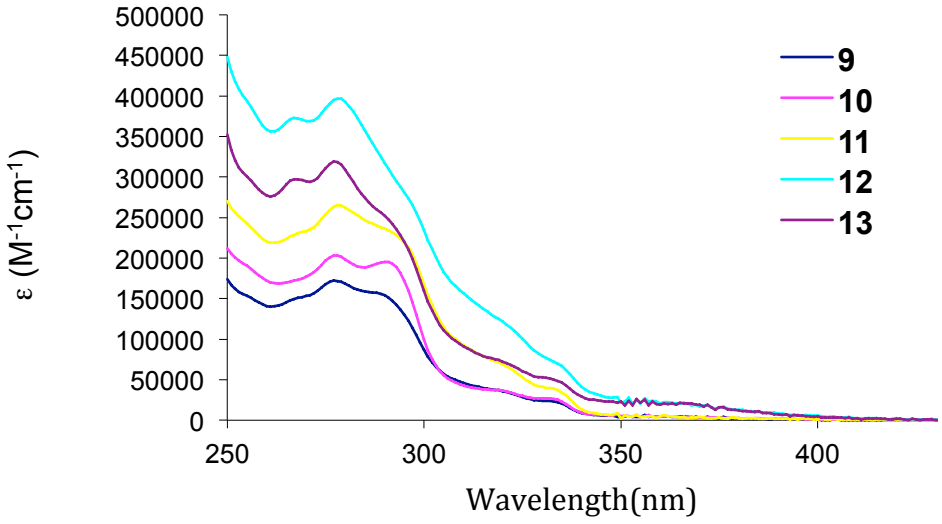


**Figure S46.** Absorption spectra of dichloromethane solutions of compounds **9 -13**.

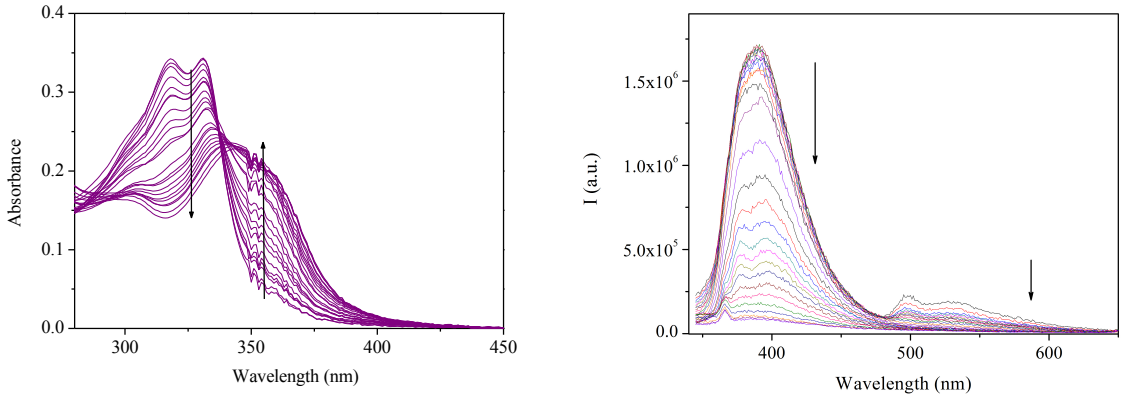


**Figure S47.** Absorption (left) and emission (right) spectra of a $10^{-6}$M dichloromethane solution of **4** upon addition of different amounts of $[Cu(CH_3CN)_4]BF_4$.

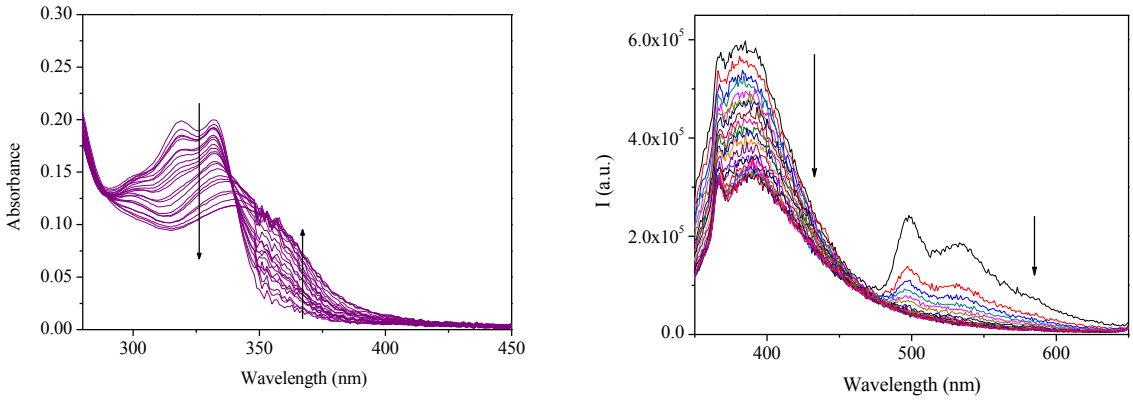


**Figure S48.** Absorption (left) and emission (right) spectra of a $10^{-6}$M dichloromethane solution of **6** upon addition of different amounts of $[Cu(CH_3CN)_4]BF_4$.

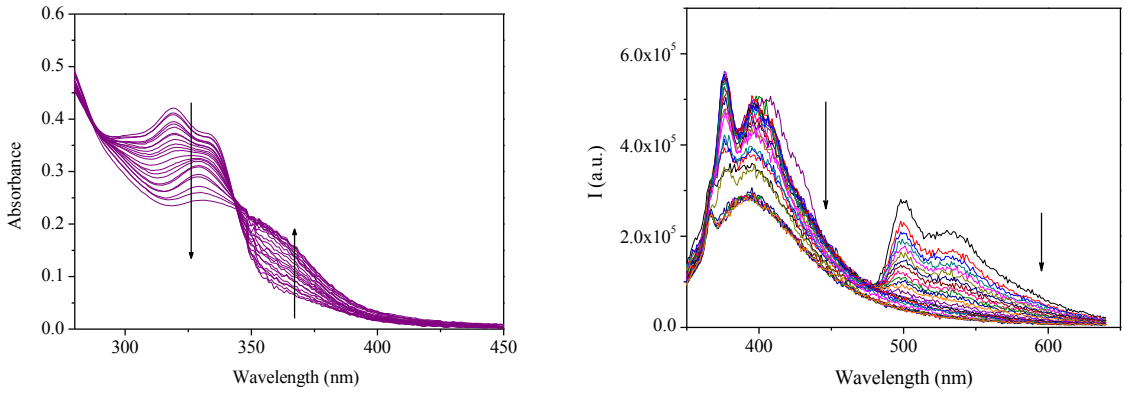


**Figure S49.** Absorption (left) and emission (right) spectra of a $10^{-6}$M dichloromethane solution of **7** upon addition of different amounts of $[Cu(CH_3CN)_4]BF_4$.

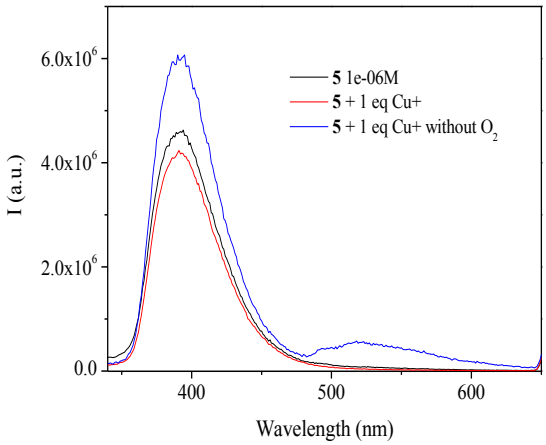


**Figure S50.** Emission spectra of $1 \cdot 10^{-6}$M dichloromethane solution of **5** in the presence of one equivalent of $[Cu(CH_3CN)_4]BF_4$ with and without oxygen.

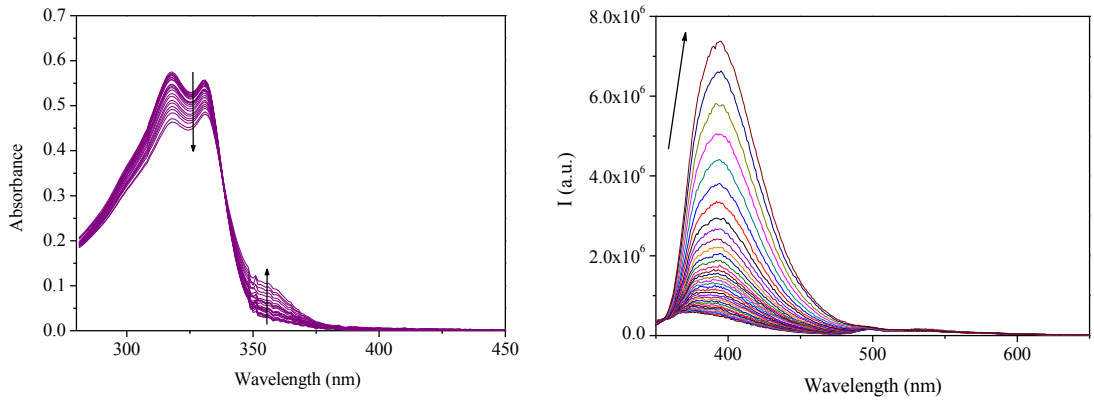


**Figure S51.** Absorption (left) and emission (right) spectra of a $10^{-6}$M dichloromethane solution of **4** upon addition of different amounts of $Zn^{2+}$.

**Table S1.** Crystal Data and Structure Refinement for $[Au_4(C{\equiv}CC_{10}H_7N_2)_4(\mu_4\text{-tetraphos})]$ (**6**) and $[Au_4(C{\equiv}CC_{10}H_7N_2)_4(\mu_4\text{-tpbz})]$ (**7**).

| | **6**·1.75$CH_2Cl_2$ | **7** |
|---|---|---|
| Formula | $C_{411}\,H_{318}\,Au_{16}\,Cl_{14}\,N_{32}$ | $C_{102}H_{70}Au_4N_8P_4$ |
| Fw | 9848.24 | 2319.4 |
| T (K) | 120 | 200(2) |
| λ (Å) | 1.54184 | 0.71073 |
| Crystal system | monoclinic | orthorhombic |
| Space group | *P2₁/c* | *Pbcn* |
| a (Å) | 33.1673(9) | 18.968(6) |
| b (Å) | 17.3472(5) | 26.452(8) |
| c (Å) | 34.8570(14) | 20.575(1) |
| α (º) | 90 | 90 |
| β (º) | 105.877(3) | 90 |
| γ (º) | 90 | 90 |
| V (Å$^3$) | 19290.2(12) | 10323(5) |
| Z | 2 | 4 |
| $D_{calc}$ (Mg m$^{-3}$) | 1.696 | 1.492 |
| μ (mm$^{-1}$) | 13.090 | 5.774 |
| F(000) | 9500 | 4456 |
| Crystal size (mm$^3$) | 0.23 x 0.17 x 0.13 | 0.3 x 0.17 x 0.13 |
| θ (º) | 3.26-66.75 | 3.02 -23.01 |
| Index ranges | $-39 \le h \le 28$ | $-20 \le h \le 20$ |
| | $-20 \le k \le 13$ | $-28 \le k \le 29$ |
| | $-41 \le l \le 40$ | $-22 \le l \le 22$ |
| Reflections collected | 59429 | 89602 |
| Independent reflections [R(int)] | 27931 ($R_{int}$ = 0.0379) | 7185 ($R_{int}$ = 0.184) |
| GOF ($F^2$) | 1.087 | 1.13 |
| Data/restrains/parameters | 33966/183/1777 | 7185/0/196 |
| *R1*, w*R*2 (I>2σ(I)) | 0.1094, 0.2547 | 0.092, 0.222 |
| *R1*, w*R*2 (all data) | 0.1250, 0.2650 | 0.126, 0.248 |